

Electronic Supplementary Information

Tunnelling in Carbonic Acid

J. Philipp Wagner,^a Hans Peter Reisenauer,^a Viivi Hirvonen,^a Chia-Hua Wu,^b Joseph L. Tyberg,^b Wesley D. Allen,^{b,*} and Peter R. Schreiner^{a,*}

^aInstitute of Organic Chemistry, Justus-Liebig-University, Heinrich-Buff-Ring 58, D-35392 Giessen, Germany

^bCenter for Computational Quantum Chemistry and Department of Chemistry, University of Georgia, Athens, Georgia 30602, USA

prs@uni-giessen.de

wdallen@uga.edu

Table of Contents

1. Experimental Methods.....	S2
2. Matrix-Isolation Spectra.....	S3
3. Kinetic Analyses	S7
4. Theoretical Methods.....	S17
5. Geometric Structures.....	S19
6. Electronic Energies.....	S32
7. Focal Point Analyses.....	S37
8. Tunneling Computations	S46
9. Vibrational Frequencies.....	S49
10. Additional References	S51

1. Experimental Methods

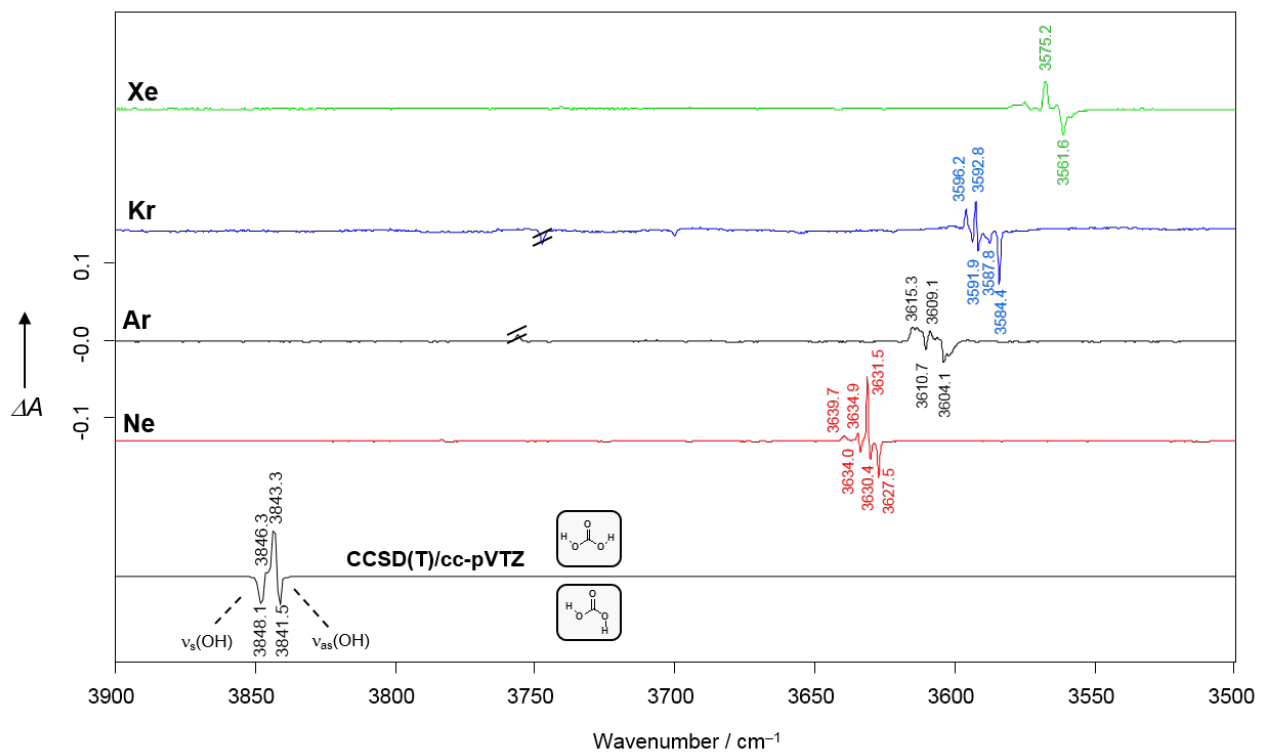
For all matrix-isolation experiments at temperatures of 12.5 K and above, an APD Cryogenics closed-cycle refrigerator system (HC-2 compressor, CS 202 coldhead) was used. The temperature was monitored by a Leybold LTC 60 Si-diode temperature controller. For experiments at 3 K, a cryostat from Sumitomo was used, which is a combination of an F-70 compressor unit and a RDK 408D2 closed-cycle refrigerator. In order to be suitable for IR measurements, a CsI window was attached to the cold fingers of the cryostats, and KBr windows were used for the outer mantle. The high-vacuum flash pyrolysis (HVFP) was performed with a small home-built water-cooled furnace that is directly connected to the vacuum shroud. The pyrolysis zone was equipped with a resistively heated, completely empty quartz tube (inner diameter 8 mm, length of heating zone 50 mm). The temperature was controlled by a Ni/CrNi thermocouple.

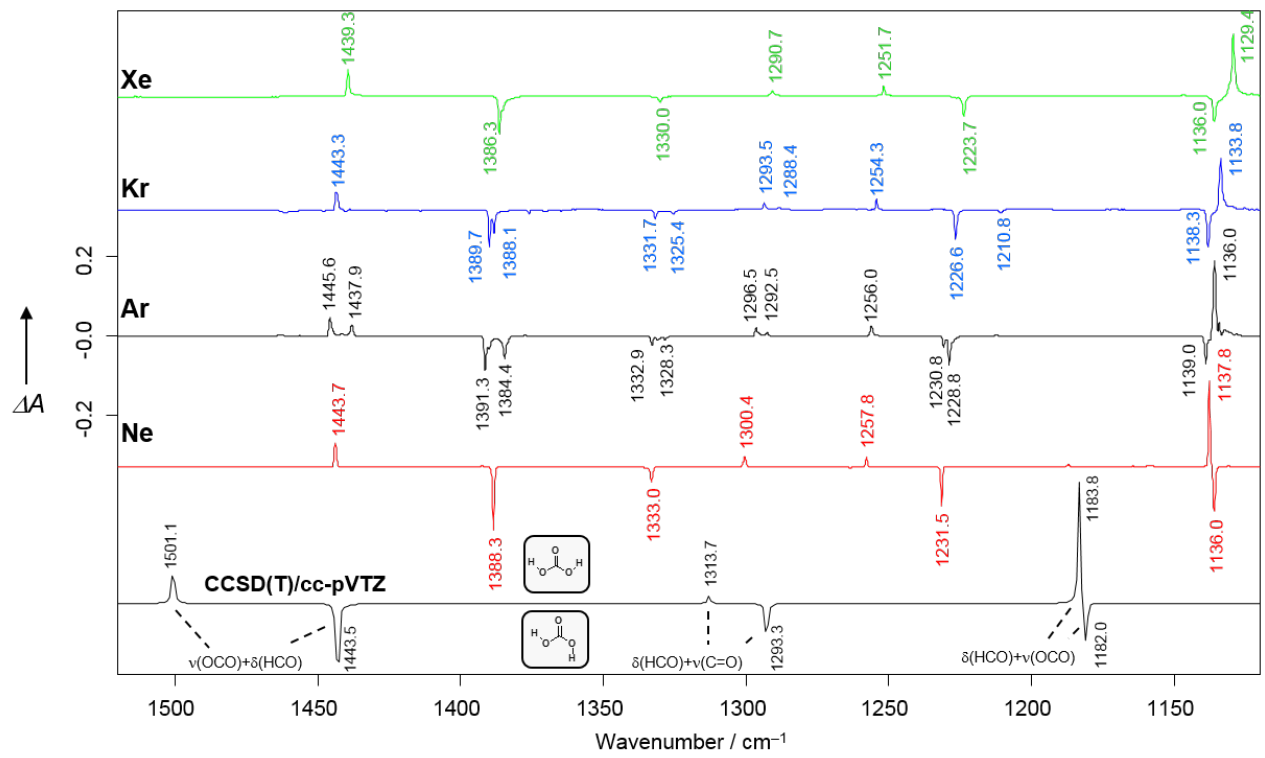
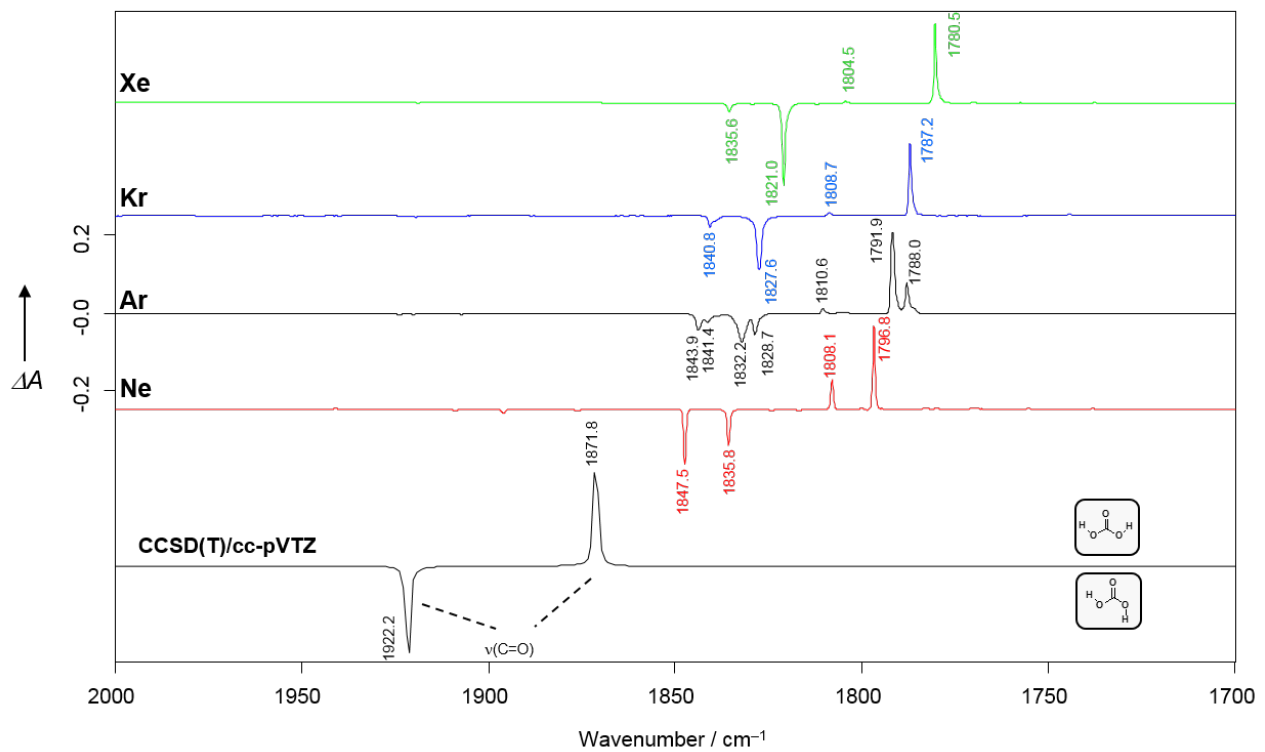
For deposition in the matrix-isolation experiments, gaseous mixtures of di-*t*-butyl carbonate in about 1000-fold excess of noble gas were prepared in a 2 L storage glass balloon. The gas mixture was pyrolyzed at a temperature of 730 °C over several hours. Narrow-band NIR irradiation was performed with an optical parametric oscillator (GWU OPO versaScan 280 MB, pump laser: Spectra-Physics Quanta Ray Nd:YAG LAB-170-10, 355 nm, line width 4 cm⁻¹). Broadband NIR irradiation of the deposited carbonic acid samples was carried out with a high-pressure mercury lamp (HBO 200, Osram) in combination with a RG850 long-pass filter. IR spectra were recorded with a Bruker Vertex 70 FTIR spectrometer, or alternatively with a Bruker IFS55 spectrometer (resolution 0.7 cm⁻¹, 50 scans collected in one measurement).

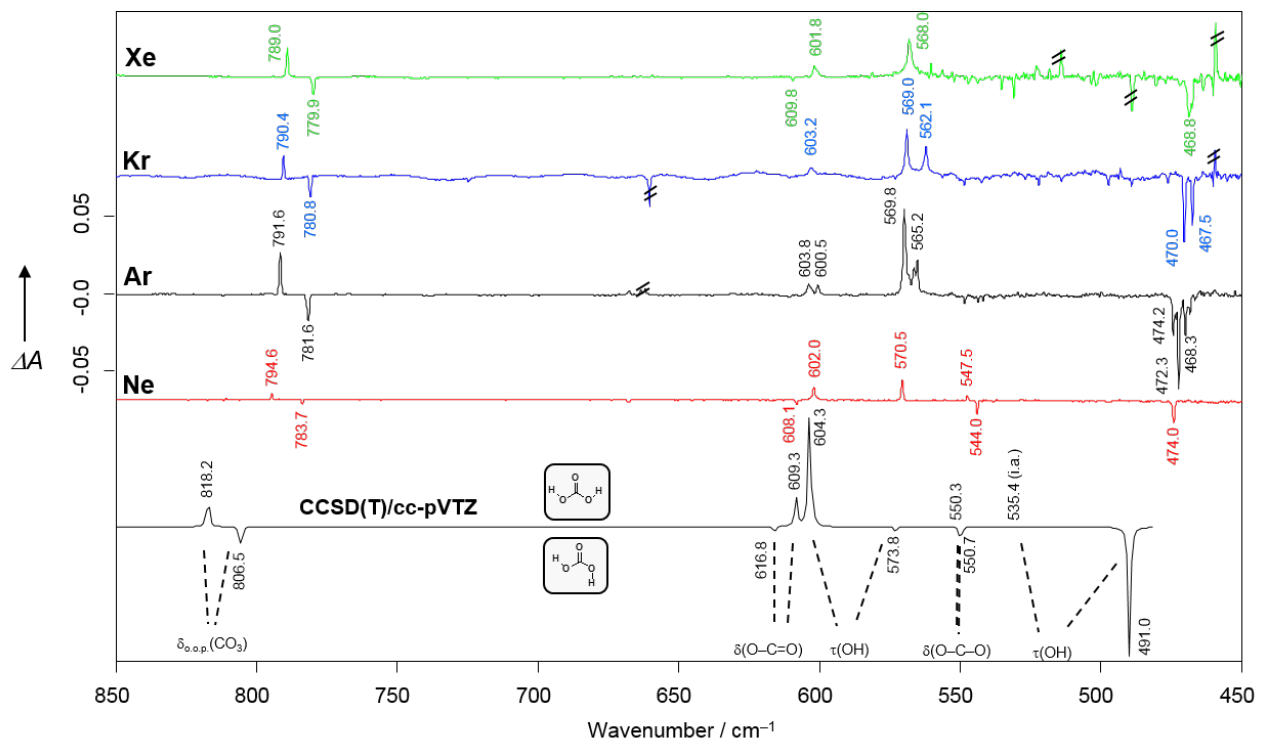
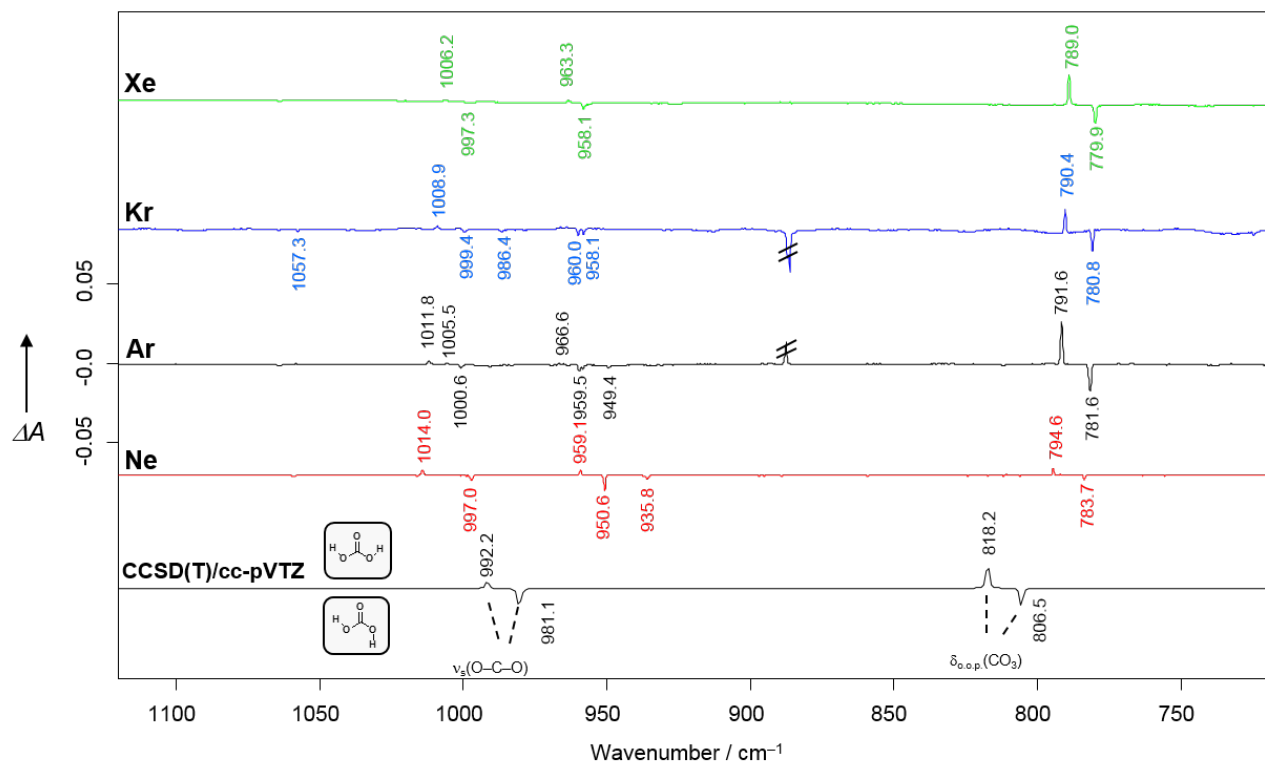
During the kinetic measurements, a long-pass IR filter (cutting off all wavelengths below 4.5 μm, LOT Oriel, 4.50 ILP-25) was used to prevent unwanted photochemistry induced by the globar. During the measurements, the matrix apparatus was not moved in order to prevent errors arising from different thicknesses of the deposited matrices.

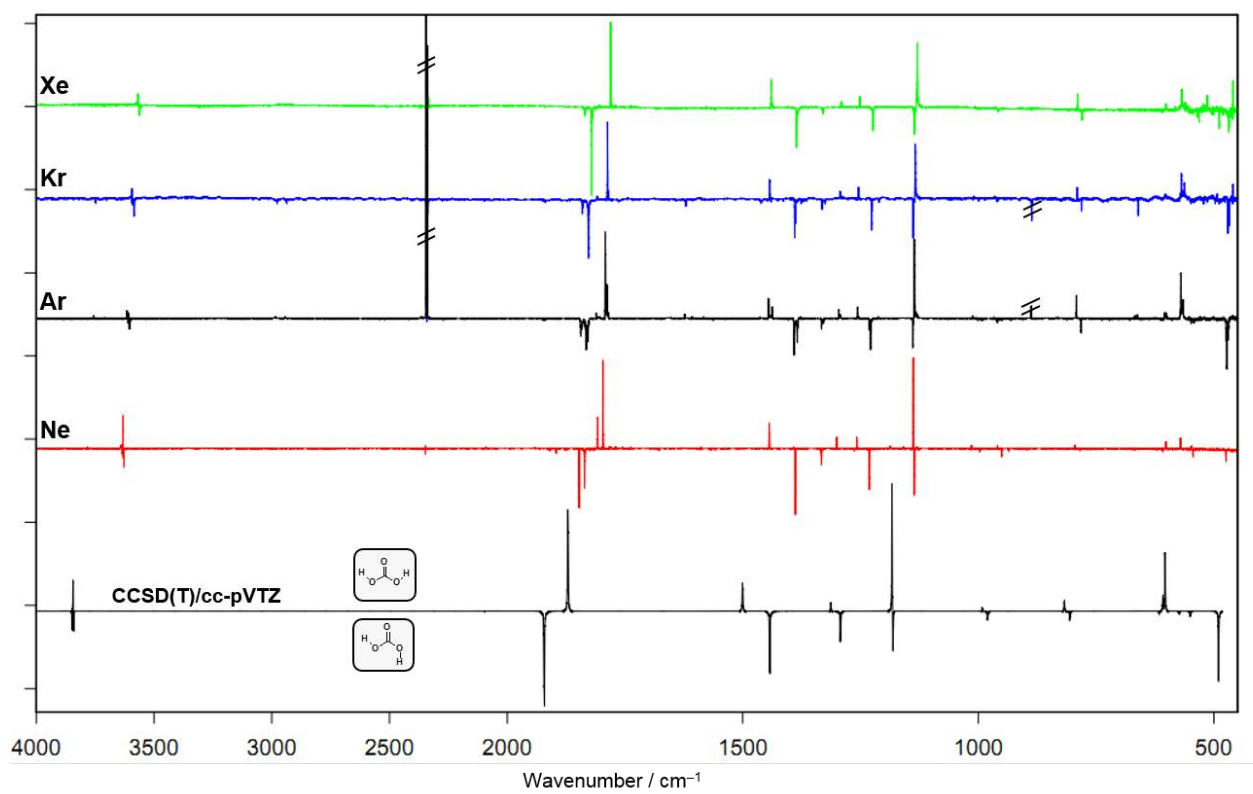
2. Matrix-Isolation Spectra

Figure S1. Difference spectra of **1cc** and **1ct** in solid noble gas matrices upon NIR irradiation generated by an optical parametric oscillator (Ne: 1406.3 nm; Ar: 2454 nm; Kr: 2467 nm; Xe: 2414 nm). Carbonic acid **1** was prepared by HVFP of gas mixtures of di-*t*-butyl carbonate in about 1000-fold excess of the corresponding noble gas. **Lower trace:** Computed IR difference spectra (unscaled CCSD(T)/cc-pVTZ harmonic vibrational frequencies) of carbonic acid conformers **1cc** (pointing upwards) and **1ct** (pointing downwards) in black; **upper traces:** Experimentally measured difference spectra of **1cc** (upwards) and **1ct** (downwards) in neon (red), argon (black), krypton (blue), and xenon (green).









3. Kinetic Analyses

A rigorous kinetic model was previously formulated¹ for a reaction cascade of n chemical species $\{A_i, i = 1, 2, \dots, n\}$



in which the i th species has m_i possible matrix sites to occupy. The differential equation for the population of species A_i in site j_i is

$$\frac{d[A_{i,j_i}]}{dt} = -k_{i,j_i}[A_{i,j_i}] + \sum_{j_{i-1}} p_{(i-1,j_{i-1}) \rightarrow (i,j_i)} k_{i-1,j_{i-1}} [A_{i-1,j_{i-1}}], \quad (2)$$

where k_{i,j_i} is the overall first-order rate constant for the loss of A_{i,j_i} , and $p_{(i-1,j_{i-1}) \rightarrow (i,j_i)}$ is the probability that decay of species A_{i-1} in site j_{i-1} to species A_i will populate site j_i . For the start of the cascade,

$$\frac{d[A_{1,j_1}]}{dt} = -k_{1,j_1}[A_{1,j_1}] \Rightarrow \quad (3)$$

$$[A_{1,j_1}] = [A_{1,j_1}]_0 e^{-k_{1,j_1} t} \quad (4)$$

for all sites j_1 . For the second species in the chain, Eq. (2) gives

$$\frac{d[A_{2,j_2}]}{dt} = -k_{2,j_2}[A_{2,j_2}] + \sum_{j_1}^{m_1} p_{(1,j_1) \rightarrow (2,j_2)} k_{1,j_1} [A_{1,j_1}]_0 e^{-k_{1,j_1} t} \quad (5)$$

The solution of this differential equation is of the form

$$[A_{2,j_2}] = [A_{2,j_2}]_0 \left(a_{j_2} e^{-k_{2,j_2} t} + \sum_{j_1}^{m_1} b_{j_1,j_2} e^{-k_{1,j_1} t} \right), \quad (6)$$

where the coefficients a_{j_2} and b_{j_1,j_2} are determined by requiring Eq. (6) to satisfy Eq. (5) for all times, including $t = 0$. The solutions for the coefficients are

$$a_{j_2} = 1 - \sum_{j_1}^{m_1} \frac{p_{(1,j_1) \rightarrow (2,j_2)} k_{1,j_1} [A_{1,j_1}]_0}{(k_{2,j_2} - k_{1,j_1}) [A_{2,j_2}]_0} \quad (7)$$

and

$$b_{j_1,j_2} = \frac{p_{(1,j_1) \rightarrow (2,j_2)} k_{1,j_1} [A_{1,j_1}]_0}{(k_{2,j_2} - k_{1,j_1}) [A_{2,j_2}]_0}. \quad (8)$$

Therefore, the overall solution for the second species in the cascade is

$$[A_{2,j_2}] = [A_{2,j_2}]_0 e^{-k_{2,j_2}t} + \sum_{j_1} [A_{1,j_1}]_0 \frac{p_{(1,j_1) \rightarrow (2,j_2)} k_{1,j_1}}{(k_{2,j_2} - k_{1,j_1})} \left(e^{-k_{1,j_1}t} - e^{-k_{2,j_2}t} \right). \quad (9)$$

This procedure can be extended to derive mathematical solutions for all species $i > 2$, but these equations are not necessary in the kinetic analysis of carbonic acid tunneling. If species 2 is the end of the cascade, then all k_{2,j_2} coefficients vanish, and

$$[A_{2,j_2}] = [A_{2,j_2}]_0 + \sum_{j_1} [A_{1,j_1}]_0 p_{(1,j_1) \rightarrow (2,j_2)} \left(1 - e^{-k_{1,j_1}t} \right). \quad (10)$$

The total populations of species 1 and 2 in all sites collectively as a function of time are

$$[A_i] = [A_i]_0 \sum_{j_1}^{m_i} f_{i,j_1}^0 e^{-k_{i,j_1}t}, \quad (11)$$

and

$$[A_2] = [A_2]_0 + [A_1]_0 \sum_{j_1}^{m_1} f_{1,j_1}^0 \left(1 - e^{-k_{1,j_1}t} \right), \quad (12)$$

where

$$f_{i,j_i}^0 = \frac{[A_{i,j_i}]_0}{[A_i]_0} \quad (13)$$

is the initial fractional occupation of species i in site j_i .

Three classes of sites for species 1 and 2

Consider the case that the manifold matrix sites of A_1 fall into three classes (1, 2, 3) – slow sites with effective rate constant $k_{1,1}$, fast sites with effective rate constant $k_{1,2}$, and frozen sites with $k_{1,3} = 0$. First, let

$$\beta_1 = \frac{[A_{1,2}]_0}{[A_{1,1}]_0}, \quad (14)$$

$$\beta_2 = \frac{[A_{1,3}]_0}{[A_{1,1}]_0}, \quad (15)$$

and

$$\gamma = \frac{[A_1]_0}{[A_2]_0}. \quad (16)$$

Application of Eqs. (11)-(13) followed by substitution with Eqs. (14)-(16) gives

$$\frac{[A_1]}{[A_1]_0} = \frac{e^{-k_{1,1}t} + \beta_1 e^{-k_{1,2}t} + \beta_2}{1 + \beta_1 + \beta_2}, \quad (17)$$

and

$$\frac{[A_2]}{[A_2]_0} = 1 + \gamma \left[1 - \frac{\left(e^{-k_{1,1}t} + \beta_1 e^{-k_{1,2}t} + \beta_2 \right)}{1 + \beta_1 + \beta_2} \right]. \quad (18)$$

Replacing the rate constants with the corresponding half-lives (τ), we arrive at

$$\frac{[A_1]}{[A_1]_0} = \frac{2^{-t/\tau_{1,1}} + 2^{-t/\tau_{1,2}} \beta_1 + \beta_2}{1 + \beta_1 + \beta_2}, \quad (19)$$

and

$$\frac{[A_2]}{[A_2]_0} = 1 + \gamma \left[1 - \frac{\left(2^{-t/\tau_{1,1}} + 2^{-t/\tau_{1,2}} \beta_1 + \beta_2 \right)}{1 + \beta_1 + \beta_2} \right]. \quad (20)$$

Eqs. (19) and (20) are suitable for fitting to the time evolution of IR absorption bands. Each equation is valid simultaneously for all IR bands of the corresponding species. In terms of the fitting parameters, the initial mole fractions of species 1 in the three classes of sites are

$$(X_{\text{fast}}, X_{\text{slow}}, X_{\text{frozen}}) = \frac{1}{1 + \beta_1 + \beta_2} (\beta_1, 1, \beta_2). \quad (21)$$

In the case that species 2 is produced by a source other than species 1, Eq. (20) should be augmented by an additional term; specifically,

$$\frac{[A_2]}{[A_2]_0} = 1 + \gamma \left[1 - \frac{\left(2^{-t/\tau_{1,1}} + 2^{-t/\tau_{1,2}} \beta_1 + \beta_2 \right)}{1 + \beta_1 + \beta_2} \right] + \gamma_f \left(1 - 2^{-t/\tau_f} \right) \quad (22)$$

where γ_f and τ_f are, respectively, the initial population ratio and decay half-life of the feeder species.

Procedure for Carbonic Acid Analysis

After NIR excitation (Table S1) experimental kinetic data measured from the matrix-isolation IR bands tabulated and characterized below (Table S2) were selected for the analysis of conformational tunneling in carbonic acid. The measurement times for the [Ne (3 K), Ar (3 K), Ar (12.5 K), Ar (17.5 K), Ar (20 K), Kr (12.5 K), Xe (12.5 K)] spectra were (271, 223, 73, 20, 62, 56, 85) h, in order.

Table S1. Irradiation methods before kinetic measurements.

Experiment	Method
Ar (3 K)	OPO, 1414 nm, 35 min
Ar (12 K)	OPO, 1414 nm, 30 min
Ar (17.5 K)	HBO200 with RG850 long-pass filter, 3 h
Ar (20 K)	OPO, 1414 nm, 45 min
Ne (3 K)	OPO, 1407.7 nm, 55 min
Kr (12.5 K)	OPO, 1423.6 nm, 30 min
Xe (12.5 K)	OPO, 1433.2 nm, 30 min

Table S2. Infrared bands^a used for kinetic analysis of conformational tunneling in carbonic acid

	1ct conformer	1cc conformer
Ne (3 K)	(1845.5–1848.5 cm ⁻¹ , 1 peak) (1833–1838 cm ⁻¹ , 1 peak) (1386–1390 cm ⁻¹ , 1 peak) (1230–1233 cm ⁻¹ , 1 peak) (1134.6–1136.65 cm ⁻¹ , 1 peak)	(1805.5–1810 cm ⁻¹ , 1 peak) (1794–1799, 1 peak) (1441.8–1445 cm ⁻¹ , 1 peak) (1136.65–1139 cm ⁻¹ , 1 peak)
Ar (3 K)	(1825.5–1835 cm ⁻¹ , 2 peaks) (1388–1394 cm ⁻¹ , 1 peak, 1 shoulder) (1382–1388 cm ⁻¹ , 1 peak, 1 shoulder) (1226–1233 cm ⁻¹ , 2 peaks, 2 shoulders)	(1784.5–1795, 2 peaks, 1 shoulder, 2 static) (1436–1440 cm ⁻¹ , 1 peak) (1254–1258 cm ⁻¹ , 1 peak) (790–792.6 cm ⁻¹ , 1 peak)
Ar (12.5 K)	(1825.7–1836 cm ⁻¹ , 2 peaks) (1388–1393.5 cm ⁻¹ , 1 peak, 2 static) (1226–1232.5 cm ⁻¹ , 3 peaks, 1 shoulder)	(1784.5–1794, 2 peaks, 2 static) (1436–1440 cm ⁻¹ , 1 peak, 1 shoulder) (1254–1258 cm ⁻¹ , 1 peak) (1133–1137.2 cm ⁻¹ , 1 peak) (790.5–792.6 cm ⁻¹ , 2 peaks)
Ar (17.5 K)	(1825.5–1835 cm ⁻¹ , 2 peaks, 1 static) (1388–1394 cm ⁻¹ , 1 peak, 2 static) (1382–1388 cm ⁻¹ , 1 peak, 2 static) (1226–1233 cm ⁻¹ , 3 peaks, 1 shoulder)	(1784.5–1795, 2 peaks, 2 static) (1254–1258 cm ⁻¹ , 1 peak) (1133–1137 cm ⁻¹ , 1 peak) (790–792.6 cm ⁻¹ , 2 peaks)
Ar (20 K)	(1825.5–1835 cm ⁻¹ , 3 peaks)	(1784.5–1795, 3 peaks),

	(1382–1388 cm ⁻¹ , 1 peak, 1 static) (1226–1233 cm ⁻¹ , 3 peaks)	(1436–1440, 1 peak) (1254–1258 cm ⁻¹ , 2 peaks) (1133–1137 cm ⁻¹ , 2 peaks) (790–792.6 cm ⁻¹ , 1 peak, 1 shoulder)
Kr (12.5 K)	(1825.5–1829 cm ⁻¹ , 1 peak) (1387–1391 cm ⁻¹ , 2 peaks) (1223–1229 cm ⁻¹ , 1 peak)	(1784–1789, 1 peak) (1131.5–1135 cm ⁻¹ , 1 peak)
Xe (12.5 K)	(1818–1823.5 cm ⁻¹ , 1 peak) (1383–1389 cm ⁻¹ , 1 peak)	(1777–1783, 1 peak) (1125–1133.5 cm ⁻¹ , 1 peak, 1 shoulder)

^aThe intensities of the peaks are time-dependent unless labeled as “static”.

In the kinetic equations above we set $A_1 = \mathbf{1ct}$ and $A_2 = \mathbf{1cc}$. The **1tt** conformer is too short-lived to be monitored in the experiments and is assumed to have already decayed to either **1ct** or **1cc**. IR band intensities were determined by numerical integration over the ranges given in the table above. Baselines were set by the absorptions at the endpoints of the ranges. The slow components of the bands make it impossible to follow the decay long enough to reach the asymptotes. The area under each band will not decay to zero at infinite time if constant absorptions from contaminants are present and/or some carbonic acid molecules are trapped in frozen sites that preclude tunneling. Therefore, the measured intensity $I_{ij}(t)$ of each band j of species i was reduced by a time-independent shift s_{ij} before execution of the kinetic analysis. These shifts were determined by minimizing the quantity

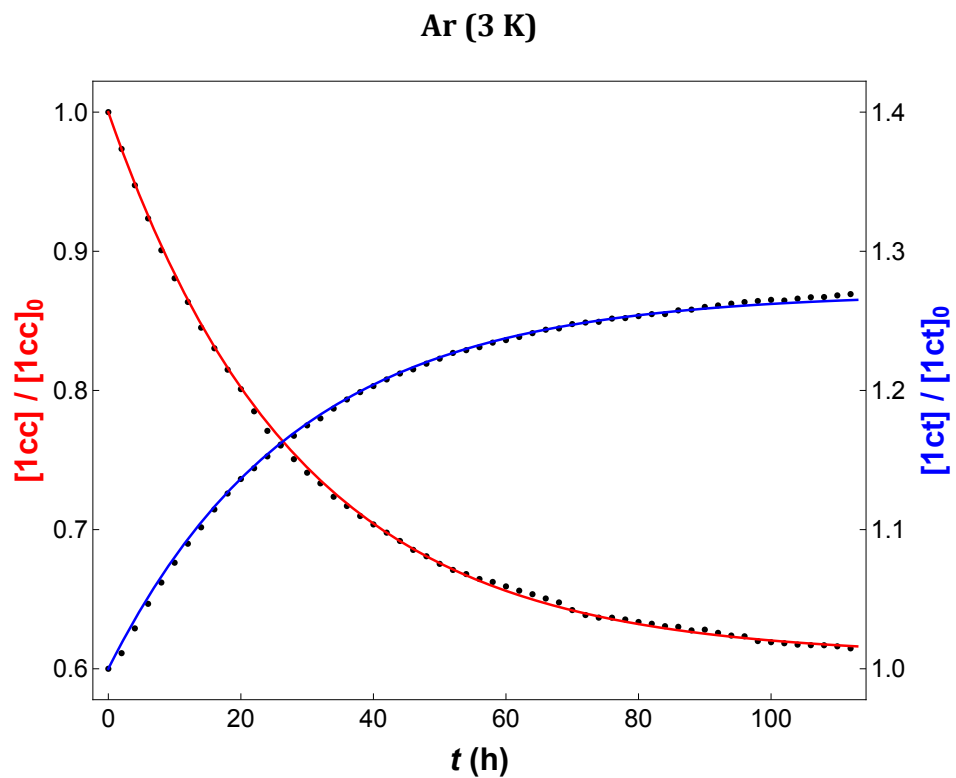
$$S_i = \sum_{j < k} \sum_m \left(\frac{I_{ij}(t_m) - s_{ij}}{I_{ij}(0) - s_{ij}} - \frac{I_{ik}(t_m) - s_{ik}}{I_{ik}(0) - s_{ik}} \right)^2, \quad (23)$$

where the sums run over all times t_m and all pairs of bands (j,k) for which measurements were made for species i . This approach produced a remarkable consistency of the kinetic data from the various bands of each conformer and yielded optimized s_{ij} parameters in accord with visual inspection of the decay and purity of the bands. To construct the final data set for fitting the kinetics, the relative intensities from all bands of a given species were averaged for each time t_m .

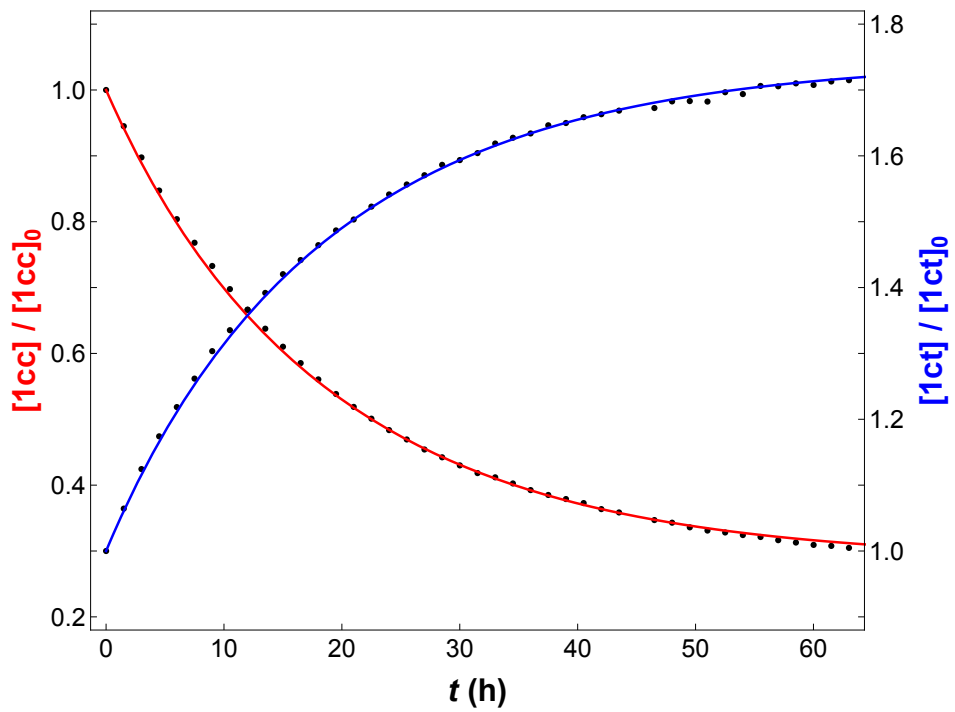
Preliminary fits of the IR bands showed that the decay profiles are generally multiexponential. Excellent fits of the data within the experimental error bars were achieved by adopting the (slow, fast, frozen) model of matrix sites specified above. Plots of the data and fits are shown in Figs. S2 below. The final kinetic analysis employed Eqs. (19) and (20) with two half-lives ($\tau_{1,1}, \tau_{1,2}$) and three population ratios (β_1, β_2, γ) as fitting parameters in a *global* nonlinear least-squares fit. In the case of Ar at 17.5 K and 20 K, the data do not

support the existence of frozen sites, so that the final fit set $\beta_2 = 0$. Likewise, for Ar at 3 K the presence of a fast tunneling component is not apparent, and the constraint $\beta_1 = 0$ was set in the final analysis. Finally, for Ne at 3K it was necessary to include a feeder species with $\tau_f = 9.3(7)$ h and $\gamma_f = 0.14(1)$ in Eq. (22) to obtain a satisfactory fit of the data.

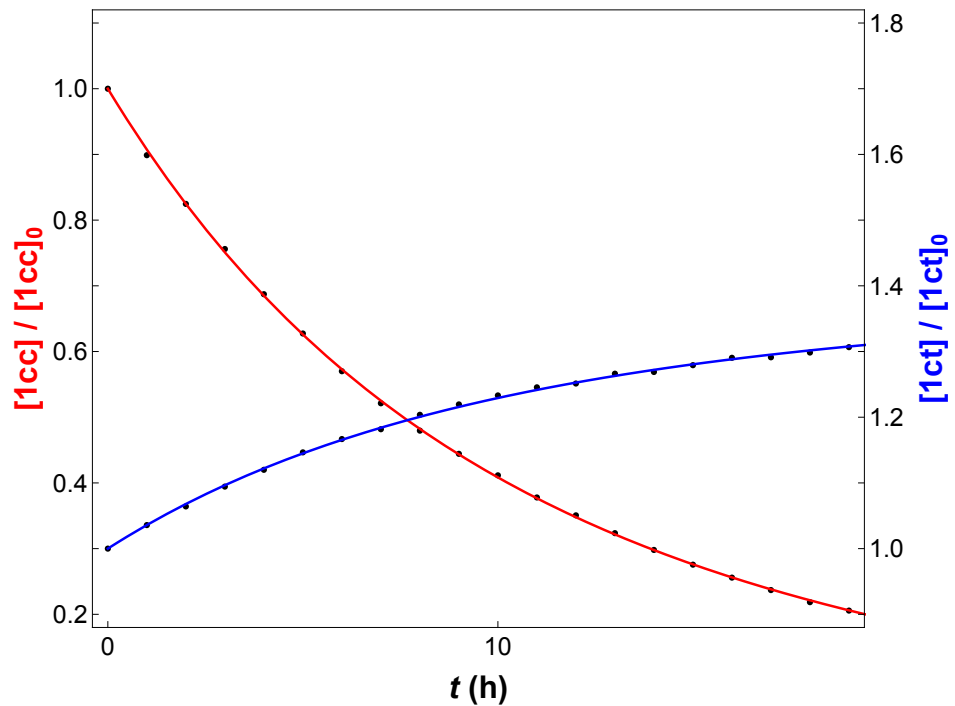
Figs. S2. Time evolution and kinetic fits of the relative populations of the **cc** and **ct** conformers of carbonic acid in various matrices. The plotted points are derived from an average of the intensities of the multiple matrix-isolation IR bands specified in Table S2, after determination of the infinite-time asymptotes via Eq. (23).



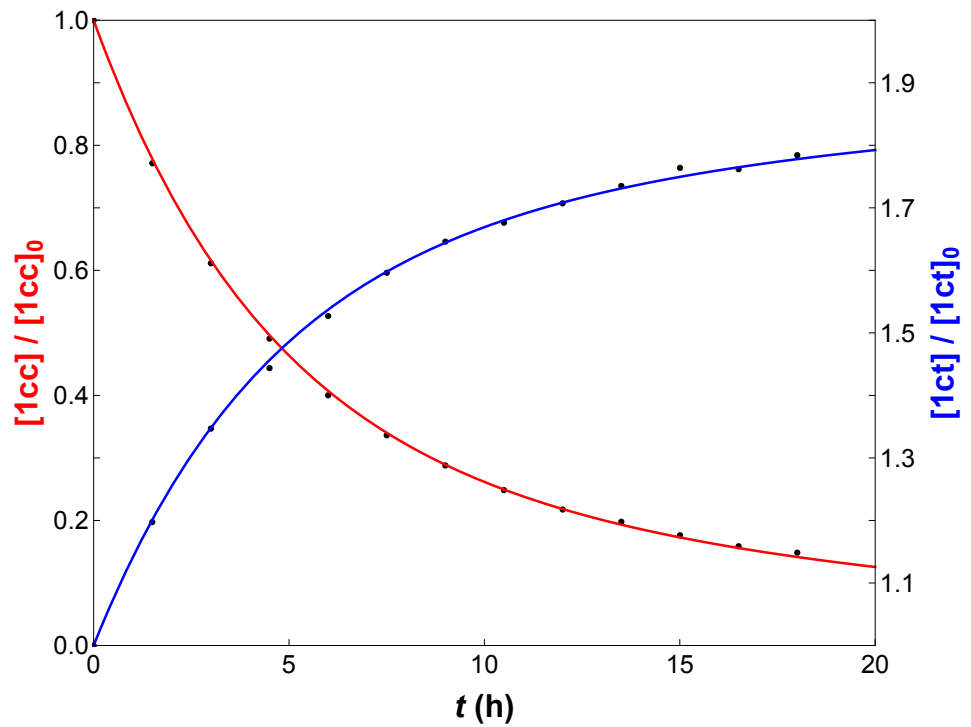
Ar (12.5 K)



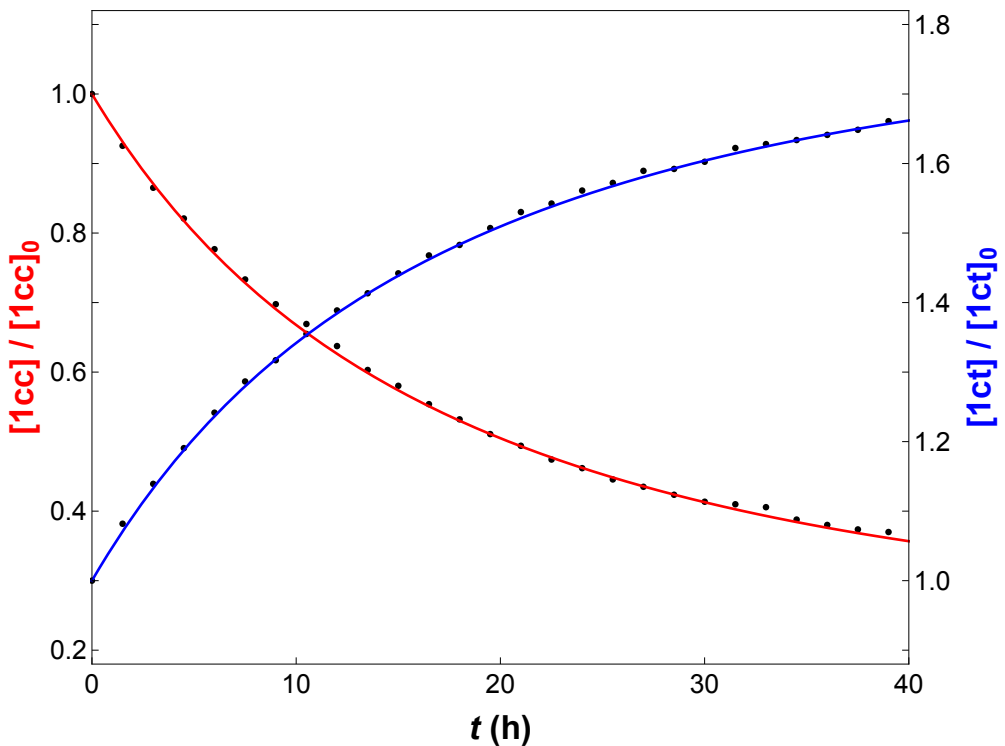
Ar (17.5 K)



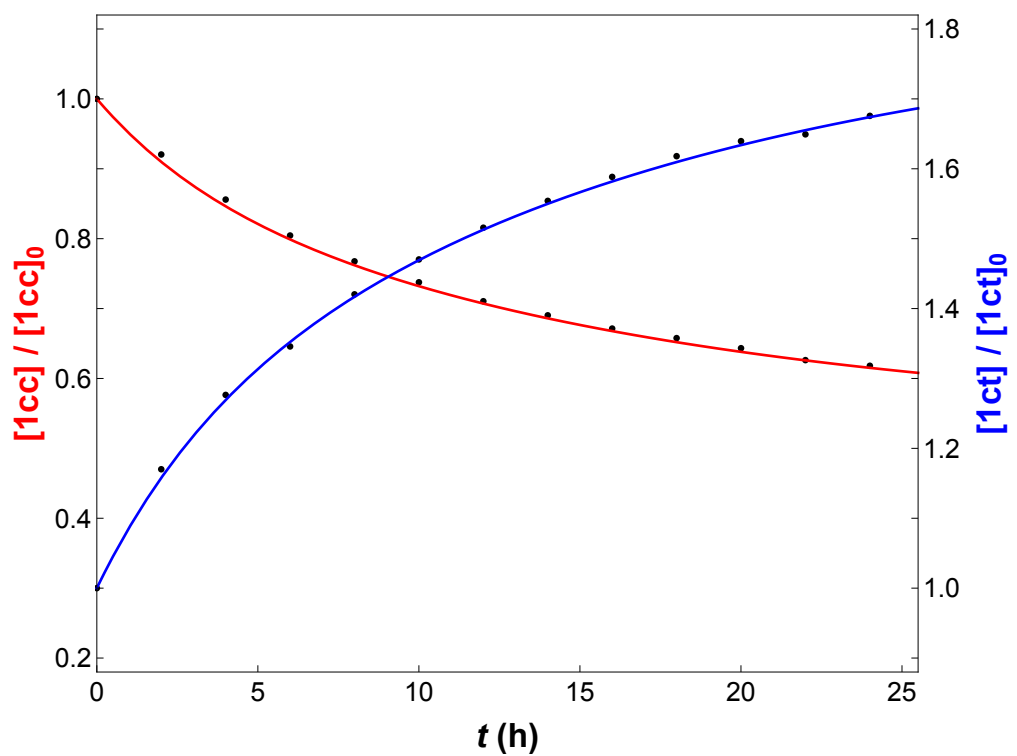
Ar (20 K)



Kr (12.5 K)

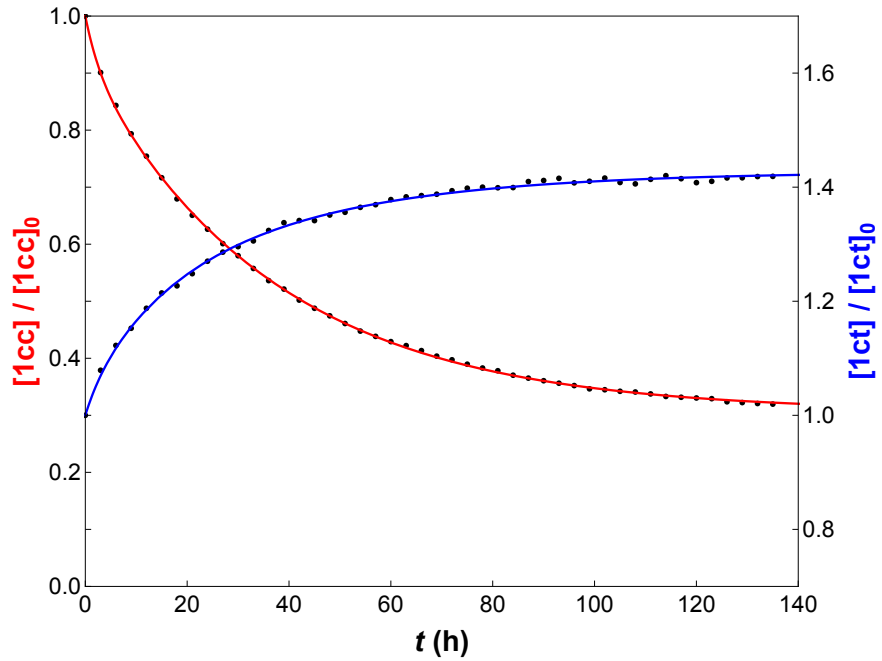


Xe (12.5 K)



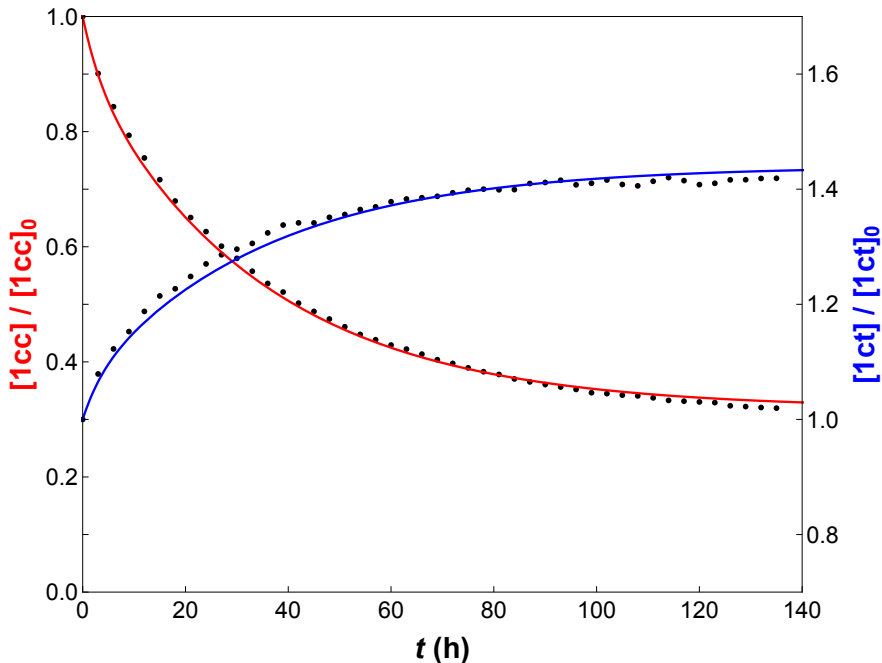
Ne (3 K)

Fit with inclusion of feeder species: $\tau_f = 9.3(7)$ h, $\gamma_f = 0.14(1)$



Ne (3 K)

Fit without inclusion of feeder species



4. Theoretical Methods

Focal Point Analysis. For the computations^{2,3} presented here, we mainly utilized coupled-cluster theory with iteratively included single and double excitations (CCSD) and perturbatively included triple excitations [CCSD(T)].⁴⁻⁷ We optimized the reference geometry of **TS1** and **TS2** at the frozen core (FC) CCSD(T)/cc-pVQZ level of theory with the core-orbitals omitted from the correlation treatment. At these structures we applied the focal-point analysis (FPA) of Allen and coworkers, aiming for energies of CCSD(T)/CBS quality.^{8,9} We computed single point energies on top of that structure employing Dunning's correlation consistent basis set families cc-pVXZ and cc-pCVXZ (with X = D(2), T(3), Q(4), 5) to converge the energy to the basis set limit.^{10,11} The RHF-energy was extrapolated with Feller's¹² exponential function:

$$E_{RHF}(X) = E_{SCF}^{\infty} + a \cdot e^{-bX}$$

The correlation energy was extrapolated from two points on the basis of a power law:^{13,14}

$$E_{corr}(X) = E_{corr}^{\infty} + b \cdot X^{-3}$$

Core correlation was accounted for by the following approximation:

$$\Delta E_{core} = E_{AE-CCSD(T)}^{cc-pCVTZ} - E_{FC-CCSD(T)}^{cc-pCVTZ}, \text{ where AE denotes the correlation of all electrons}$$

Mass velocity contributions and one-electron Darwin terms (MVD1)¹⁵ were computed at the CCSD(T)/cc-pVTZ level of theory to assess relativistic effects. The diagonal Born-Oppenheimer correction (DBOC)¹⁶ was computed at the HF/cc-pVTZ level. CCSD(T)/cc-pVTZ harmonic vibrational frequencies were computed at the corresponding optimized structures to obtain zero-point vibrational energies (ZPVEs) and confirm that the stationary points were true transition states.

The distinguished reaction path (DRP) for the **1ct** → **1cc** isomerization was constructed by MP2/aug-cc-pVTZ constrained geometry optimizations using the $\tau_{O-C-O-H}$ torsion angle as the reaction coordinate. The zero-point energy corrections [Δ (ZPVE)] along the path were evaluated using the DRP vibrational projection scheme of Allen *et al.*¹⁷ Focal point analyses were performed to compute the final energy curve along the DRP. The FPA procedure included complete basis set (CBS) extrapolation of Hartree-Fock energies and

MP2 electron correlation energies ($\varepsilon_{\text{corr}}^{\text{MP2}}$) using cc-pVXZ (T, Q, 5) basis sets and the equations above.

For the final DRP energy curve, CCSD(T)/CBS energies were then obtained from the composite (c~) scheme:

$$E_{\text{c-CBS}}^{\text{CCSD(T)}} = E_{\text{CBS}}^{\text{HF}} + \varepsilon_{\text{CBS}}^{\text{MP2}} + (E_{\text{cc-pVQZ}}^{\text{CCSD(T)}} - E_{\text{cc-pVQZ}}^{\text{MP2}})$$

Core correlation corrections [$\Delta(\text{core})$] to the valence $E_{\text{c-CBS}}^{\text{CCSD(T)}}$ energies were evaluated by differencing all-electron and frozen-core results at the CCSD(T)/cc-pCVTZ level of theory.

5. Geometric Structures

Table S3. Cartesian coordinates (in Å) of FC-CCSD(T)/cc-pVQZ structures

TS1			
	X	Y	Z
H	-1.206540474	1.319753687	0.733612327
O	-1.108223077	0.779104272	-0.058380438
C	0.298684086	-0.093320519	-0.004128863
O	1.343425346	0.436504221	-0.000055791
O	-0.302743172	-1.201826415	0.011933720
H	-1.277916579	-0.427333865	0.053577842

TS2			
	X	Y	Z
H	-1.444450532	-0.101112506	0.0000000000
O	-0.612376830	-1.090587653	0.0000000000
C	0.025917191	0.014839411	0.0000000000
O	-0.757301952	1.007985762	0.0000000000
O	1.333866807	0.125956150	0.0000000000
H	1.704221008	-0.763641353	0.0000000000

H ₂ O			
	X	Y	Z
H	0.0000000000	-0.755423537	0.523057214
O	0.0000000000	0.0000000000	-0.065914720
H	0.0000000000	0.755423537	0.523057214

CO ₂			
	X	Y	Z
O	0.0000000000	0.0000000000	1.162625827
C	0.0000000000	0.0000000000	0.0000000000
O	0.0000000000	0.0000000000	-1.162625827

Table S4. Cartesian coordinates (in Å) of FC-CCSD(T)/cc-pVTZ structures

TS1			
	X	Y	Z
H	-1.200726816	1.306348251	0.748573385
O	-1.107765323	0.784775750	-0.058913308
C	0.298439469	-0.093486416	-0.004567170
O	1.348818059	0.432707956	0.000064972
O	-0.308858424	-1.203124513	0.011980668
H	-1.276615342	-0.421112412	0.049630963

TS2			
	X	Y	Z
H	-1.442240725	-0.101543986	0.0000000000
O	-0.614009712	-1.092596462	0.0000000000
C	0.026263792	0.014938245	0.0000000000
O	-0.759838574	1.009705969	0.0000000000
O	1.337756297	0.126432187	0.0000000000
H	1.702328321	-0.767361336	0.0000000000

H₂O			
	X	Y	Z
H	0.0000000000	-0.753879329	0.527020397
O	0.0000000000	0.0000000000	-0.066414153
H	0.0000000000	0.753879329	0.527020397

CO₂			
	X	Y	Z
O	0.0000000000	0.0000000000	1.166288495
C	0.0000000000	0.0000000000	0.0000000000
O	0.0000000000	0.0000000000	-1.166288495

Table S5. Cartesian coordinates (in Å) of MP2/aug-cc-pVTZ structures

TS2			
	X	Y	Z
6	0.0000000000	0.034075000	0.0000000000
8	-0.159073000	-1.237164000	0.0000000000
8	1.226123000	0.362157000	0.0000000000
8	-0.978428000	0.914196000	0.0000000000
1	-1.812240000	0.423345000	0.0000000000
1	1.103265000	-0.941303000	0.0000000000

Figure S3. Illustrations (in Å, deg) of FC-CCSD(T)/cc-pVQZ structures

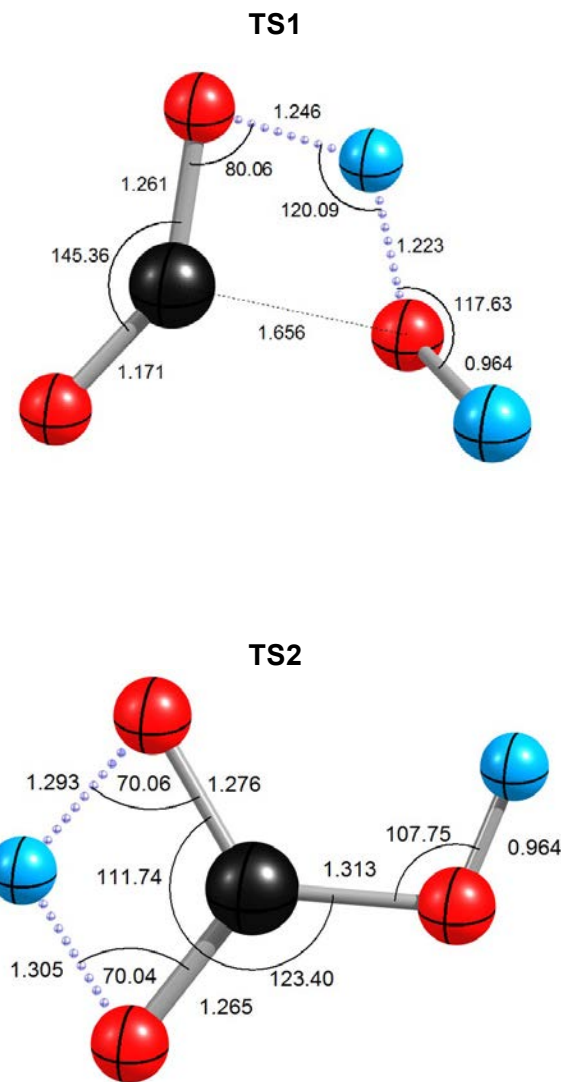
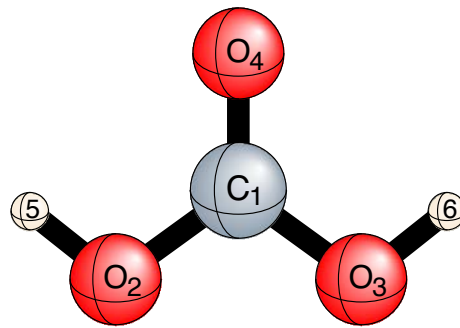


Table S6. Internal coordinates (\AA , deg) for optimized MP2/aug-cc-pVTZ geometric structures along the **1ct**→**1cc** distinguished reaction path



	$\tau_{\text{O}=\text{C}-\text{O}-\text{X}}$						
	180°(1ct)	175°	170°	165°	160°	155°	150°
$R_{\text{C}_1-\text{O}_2}$	1.3572	1.3571	1.3570	1.3568	1.3565	1.3561	1.3557
$R_{\text{C}_1-\text{O}_3}$	1.3389	1.3390	1.3394	1.3400	1.3409	1.3419	1.3432
$\theta_{\text{O}_2-\text{C}_1-\text{O}_3}$	110.382	110.381	110.3781	110.3743	110.3687	110.3624	110.3561
$R_{\text{C}_1-\text{O}_4}$	1.1992	1.1992	1.1993	1.1993	1.1993	1.1993	1.1994
$\theta_{\text{O}_4-\text{C}_1-\text{O}_3}$	125.420	125.414	125.3990	125.3745	125.3418	125.3028	125.2588
$\tau_{\text{O}_4-\text{C}_1-\text{O}_2-\text{O}_3}$	-180.000	-179.654	-179.317	-179.0031	-178.7178	-178.4762	-178.292
$R_{\text{O}_2-\text{H}_5}$	0.9672	0.9672	0.9672	0.9672	0.9673	0.9674	0.9675
$\theta_{\text{H}_5-\text{O}_2-\text{C}_1}$	105.985	105.982	105.9735	105.9633	105.9500	105.9364	105.9236
$\tau_{\text{H}_5-\text{O}_2-\text{C}_1-\text{O}_4}$	-0.000	-0.208	-0.4113	-0.6034	-0.7501	-0.8568	-0.9213
$R_{\text{O}_3-\text{H}_6}$	0.9663	0.9663	0.9663	0.9662	0.9661	0.9660	0.9658
$\theta_{\text{H}_6-\text{O}_3-\text{C}_1}$	108.497	108.500	108.5088	108.5261	108.5528	108.5935	108.6493
$\tau_{\text{H}_6-\text{O}_3-\text{C}_1-\text{O}_4}$	180.000	175.000	170.0000	165.0000	160.0000	155.0000	150.0000

	$\tau_{\text{O}=\text{C}-\text{O}-\text{X}}$						
	145°	140°	135°	130°	125°	120°	115°
$R_{\text{C}_1-\text{O}_2}$	1.3551	1.3544	1.3537	1.3529	1.3520	1.3511	1.3501
$R_{\text{C}_1-\text{O}_3}$	1.3447	1.3463	1.3480	1.3499	1.3518	1.3536	1.3554
$\theta_{\text{O}_2-\text{C}_1-\text{O}_3}$	110.3496	110.3425	110.3335	110.3207	110.3012	110.2712	110.2259
$R_{\text{C}_1-\text{O}_4}$	1.1994	1.1995	1.1995	1.1996	1.1997	1.1998	1.1999
$\theta_{\text{O}_4-\text{C}_1-\text{O}_3}$	125.2124	125.1661	125.1219	125.0815	125.0463	125.0166	124.9923
$\tau_{\text{O}_4-\text{C}_1-\text{O}_2-\text{O}_3}$	-178.180	-178.157	-178.2342	-178.4244	-178.7347	-179.1671	-179.717
$R_{\text{O}_2-\text{H}_5}$	0.9676	0.9677	0.9678	0.9679	0.9680	0.9681	0.9682
$\theta_{\text{H}_5-\text{O}_2-\text{C}_1}$	105.9133	105.9066	105.9037	105.9042	105.9075	105.9122	105.9169
$\tau_{\text{H}_5-\text{O}_2-\text{C}_1-\text{O}_4}$	-0.9469	-0.9393	-0.9055	-0.8526	-0.7867	-0.7120	-0.6309
$R_{\text{O}_3-\text{H}_6}$	0.9656	0.9655	0.9653	0.9650	0.9648	0.9646	0.9644
$\theta_{\text{H}_6-\text{O}_3-\text{C}_1}$	108.7230	108.8151	108.9249	109.0507	109.1889	109.3343	109.4798
$\tau_{\text{H}_6-\text{O}_3-\text{C}_1-\text{O}_4}$	145.0000	140.0000	135.0000	130.0000	125.0000	120.0000	115.0000

	110°	105°	100°	95°	90°	85°	80°
	τ₀=C-O-X						
$R_{C_1-O_2}$	1.3491	1.3482	1.3473	1.3465	1.3457	1.3450	1.3443
$R_{C_1-O_3}$	1.3569	1.3583	1.3593	1.3600	1.3603	1.3602	1.3597
$\theta_{O_2-X_1-O_3}$	110.1604	110.0708	109.9542	109.8107	109.6433	109.4575	109.2609
$R_{C_1-O_4}$	1.2001	1.2003	1.2006	1.2009	1.2013	1.2017	1.2021
$\theta_{O_4-C_1-O_3}$	124.9732	124.9585	124.9476	124.9404	124.9376	124.9407	124.9515
$\tau_{O_4-C_1-O_2-O_3}$	179.6276	178.8887	178.0945	177.2792	176.4795	175.7306	175.0637
$R_{O_2-H_5}$	0.9683	0.9683	0.9684	0.9684	0.9684	0.9684	0.9684
$\theta_{H_5-O_2-C_1}$	105.9200	105.9203	105.9167	105.9087	105.8960	105.8793	105.8590
$\tau_{H_5-O_2-C_1-O_4}$	-0.5440	-0.4509	-0.3493	-0.2371	-0.1111	0.0286	0.1827
$R_{O_3-H_6}$	0.9642	0.9641	0.9639	0.9638	0.9638	0.9638	0.9638
$\theta_{H_6-O_3-C_1}$	109.6154	109.7303	109.8129	109.8518	109.8384	109.7671	109.6367
$\tau_{H_6-O_3-C_1-O_4}$	110.0000	105.0000	100.0000	95.0000	90.0000	85.0000	80.0000

	75°	70°	65°	60°	55°	50°	45°
	τ₀=C-O-X						
$R_{C_1-O_2}$	1.3438	1.3432	1.3428	1.3424	1.3420	1.3416	1.3413
$R_{C_1-O_3}$	1.3589	1.3577	1.3563	1.3547	1.3530	1.3512	1.3494
$\theta_{O_2-X_1-O_3}$	109.0625	108.8706	108.6931	108.5356	108.4023	108.2951	108.2143
$R_{C_1-O_4}$	1.2026	1.2031	1.2036	1.2041	1.2046	1.2050	1.2055
$\theta_{O_4-C_1-O_3}$	124.9721	125.0043	125.0493	125.1072	125.1774	125.2580	125.3465
$\tau_{O_4-C_1-O_2-O_3}$	174.5041	174.0699	173.7719	173.6150	173.5984	173.7178	173.9655
$R_{O_2-H_5}$	0.9683	0.9682	0.9681	0.9680	0.9679	0.9678	0.9677
$\theta_{H_5-O_2-C_1}$	105.8362	105.8122	105.7880	105.7644	105.7421	105.7217	105.7034
$\tau_{H_5-O_2-C_1-O_4}$	0.3488	0.5221	0.6959	0.8622	1.0119	1.1361	1.2261
$R_{O_3-H_6}$	0.9639	0.9641	0.9643	0.9645	0.9648	0.9651	0.9654
$\theta_{H_6-O_3-C_1}$	109.4501	109.2133	108.9347	108.6237	108.2903	107.9441	107.5945
$\tau_{H_6-O_3-C_1-O_4}$	75.0000	70.0000	65.0000	60.0000	55.0000	50.0000	45.0000

	40°	35°	30°	25°	20°	15°	10°
	τ₀=C-O-X						
$R_{C_1-O_2}$	1.3410	1.3407	1.3404	1.3402	1.3400	1.3398	1.3397
$R_{C_1-O_3}$	1.3476	1.3459	1.3443	1.3430	1.3418	1.3408	1.3402
$\theta_{O_2-X_1-O_3}$	108.1584	108.1246	108.1091	108.1077	108.1153	108.1274	108.1395
$R_{C_1-O_4}$	1.2059	1.2063	1.2067	1.2070	1.2073	1.2075	1.2077
$\theta_{O_4-C_1-O_3}$	125.4393	125.5330	125.6237	125.7076	125.7813	125.8419	125.8871
$\tau_{O_4-C_1-O_2-O_3}$	174.3315	174.8044	175.3715	176.0196	176.7351	177.5044	178.3140
$R_{O_2-H_5}$	0.9676	0.9675	0.9673	0.9673	0.9672	0.9671	0.9671
$\theta_{H_5-O_2-C_1}$	105.6874	105.6737	105.6622	105.6527	105.6451	105.6392	105.6351
$\tau_{H_5-O_2-C_1-O_4}$	1.2745	1.2753	1.2249	1.1222	0.9693	0.7711	0.5362
$R_{O_3-H_6}$	0.9656	0.9659	0.9662	0.9664	0.9666	0.9668	0.9669
$\theta_{H_6-O_3-C_1}$	107.2502	106.9198	106.6114	106.3330	106.0923	105.8963	105.7512
$\tau_{H_6-O_3-C_1-O_4}$	40.0000	35.0000	30.0000	25.0000	20.0000	15.0000	10.0000

	$\tau_{O=C-O-X}$	
	5°	$0^\circ(\mathbf{1cc})$
$R_{C_1-O_2}$	1.3396	1.3396
$R_{C_1-O_3}$	1.3397	1.3396
$\theta_{O_2-X_1-O_3}$	108.1483	108.1517
$R_{C_1-O_4}$	1.2078	1.2078
$\theta_{O_4-C_1-O_3}$	125.9147	125.9241
$\tau_{O_4-C_1-O_2-O_3}$	179.1509	180.0000
$R_{O_2-H_5}$	0.9670	0.9670
$\theta_{H_5-O_2-C_1}$	105.6326	105.6318
$\tau_{H_5-O_2-C_1-O_4}$	0.2739	0.0000
$R_{O_3-H_6}$	0.9670	0.9670
$\theta_{H_6-O_3-C_1}$	105.6637	105.6317
$\tau_{H_6-O_3-C_1-O_4}$	5.0000	0.0000

Table S7. Cartesian coordinates (bohr) for optimized MP2/aug-cc-pVTZ geometric structures along the **1ct→1cc** distinguished reaction path

$\tau_{O=C-O-X} = 180^\circ$ (1ct)			
	X	Y	Z
C	-0.17261908	0.14447888	0.00000000
O	-0.02568014	-2.41601464	0.00000000
O	2.14478293	1.16012283	0.00000000
O	-2.09164575	1.34991968	0.00000000
H	-1.75094522	-3.01914617	0.00000000
H	3.37052805	-0.19342958	0.00000000

$\tau_{O=C-O-X} = 175^\circ$			
	X	Y	Z
C	-0.17181022	-0.14536119	0.00551395
O	-0.03925347	2.41584116	0.00287312
O	2.15147959	-1.14802364	0.00767236
O	-2.0841164	-1.3614059	-0.00526679
H	-1.76784078	3.00917509	-0.01559469
H	3.36743392	0.2069314	-0.13383568

$\tau_{O=C-O-X} = 170^\circ$			
	X	Y	Z
C	-0.16938412	-0.14794537	0.01092513
O	-0.07951455	2.41487536	0.00565623
O	2.17095158	-1.11190877	0.01533369
O	-2.06141288	-1.39521772	-0.01042397
H	-1.8176258	2.97904251	-0.03086238
H	3.35794836	0.24660996	-0.26691055

$\tau_{O=C-O-X} = 165^\circ$			
	X	Y	Z
C	-0.16538059	-0.15201752	0.01608352
O	-0.14480452	2.41189721	0.00826989
O	2.20128912	-1.05262792	0.02298727
O	-2.02341639	-1.44924913	-0.01535058
H	-1.89726896	2.92850317	-0.04545903
H	3.34161096	0.30958871	-0.39849361

$\tau_{O=C-O-X} = 160^\circ$			
	X	Y	Z
C	-0.16002631	-0.15711315	0.02091143
O	-0.22974624	2.40537612	0.0105663
O	2.23847888	-0.97407805	0.03063367
O	-1.97180101	-1.51804172	-0.0199602
H	-1.99904488	2.85946221	-0.05834417
H	3.318319	0.38794174	-0.52773518

$\tau_{O-C-O-X} = 155^\circ$

	<i>X</i>	<i>Y</i>	<i>Z</i>
C	-0.15356577	-0.16274911	0.02524687
O	-0.32902408	2.39395191	0.01248893
O	2.2786366	-0.88022227	0.0382709
O	-1.90832968	-1.59626778	-0.02412956
H	-2.11526889	2.77408199	-0.06939913
H	3.28856152	0.4736841	-0.65385276

 $\tau_{O-C-O-X} = 150^\circ$

	<i>X</i>	<i>Y</i>	<i>Z</i>
C	-0.14633948	-0.16842632	0.02894027
O	-0.43647216	2.37689478	0.0139687
O	2.31805189	-0.77609358	0.04589596
O	-1.83581036	-1.67820686	-0.02774658
H	-2.2377468	2.67587595	-0.0783196
H	3.25379287	0.55803147	-0.77600458

 $\tau_{O-C-O-X} = 145^\circ$

	<i>X</i>	<i>Y</i>	<i>Z</i>
C	-0.13878383	-0.1736928	0.03182068
O	-0.54557745	2.35450346	0.01495416
O	2.35370301	-0.66751949	0.05350498
O	-1.75806888	-1.75842573	-0.03069634
H	-2.35853068	2.56991202	-0.08490891
H	3.21657012	0.63205086	-0.89329775

 $\tau_{O-C-O-X} = 140^\circ$

	<i>X</i>	<i>Y</i>	<i>Z</i>
C	-0.13130007	-0.17824443	0.03372189
O	-0.65115817	2.32785762	0.01540621
O	2.38391581	-0.55955494	0.06108492
O	-1.67886407	-1.83307072	-0.03287073
H	-2.47192126	2.46125504	-0.08904087
H	3.17995869	0.68898674	-1.00476732

 $\tau_{O-C-O-X} = 135^\circ$

	<i>X</i>	<i>Y</i>	<i>Z</i>
C	-0.12422039	-0.18192606	0.03449000
O	-0.74954200	2.29849842	0.01529832
O	2.40816848	-0.45615057	0.06861022
O	-1.60150719	-1.89985625	-0.03417307
H	-2.57444334	2.35444795	-0.09063823
H	3.14698963	0.72441437	-1.10936635

$\tau_{O=C-O-X} = 130^\circ$

	<i>X</i>	<i>Y</i>	<i>Z</i>
C	-0.11776300	-0.18471432	0.03399296
O	-0.83873378	2.26799248	0.01461722
O	2.42677753	-0.35978783	0.07603968
O	-1.52838756	-1.95797218	-0.03452404
H	-2.66472827	2.25285002	-0.08965558
H	3.12012512	0.73635849	-1.20596207

 $\tau_{O=C-O-X} = 125^\circ$

	<i>X</i>	<i>Y</i>	<i>Z</i>
C	-0.11204605	-0.18667275	0.03213599
O	-0.91791498	2.23770853	0.01336460
O	2.44046908	-0.27180230	0.08331192
O	-1.46106931	-2.00753156	-0.03386998
H	-2.74273105	2.15871728	-0.08607219
H	3.10103586	0.72458724	-1.29335109

 $\tau_{O=C-O-X} = 120^\circ$

	<i>X</i>	<i>Y</i>	<i>Z</i>
C	-0.10710758	-0.18791572	0.02887713
O	-0.98700369	2.20873177	0.01156017
O	2.45008825	-0.19272659	0.09034217
O	-1.40046136	-2.04914493	-0.03219139
H	-2.80911384	2.07341492	-0.07990280
H	3.09055003	0.69001711	-1.37029577

 $\tau_{O=C-O-X} = 115^\circ$

	<i>X</i>	<i>Y</i>	<i>Z</i>
C	-0.10292698	-0.18858372	0.02424146
O	-1.04633865	2.18185751	0.00924461
O	2.45643893	-0.12256961	0.09702143
O	-1.34698551	-2.08364132	-0.02951105
H	-2.86484491	1.99763774	-0.07121264
H	3.08870162	0.63430293	-1.43558358

 $\tau_{O=C-O-X} = 110^\circ$

	<i>X</i>	<i>Y</i>	<i>Z</i>
C	-0.09944236	-0.18882355	0.01833669
O	-1.09649335	2.15761515	0.00648251
O	2.46021118	-0.06099988	0.10321650
O	-1.30069329	-2.11192056	-0.02590078
H	-2.91098742	1.93158509	-0.06015793
H	3.09478536	0.55961057	-1.48811263

 $\tau_{O=C-O-X} = 105^\circ$

	<i>X</i>	<i>Y</i>	<i>Z</i>
C	-0.09655845	-0.18877830	0.01136570
O	-1.13822401	2.13627183	0.00336165

O	2.46196706	-0.00741961	0.10877447
O	-1.26131301	-2.13488877	-0.02148653
H	-2.94862934	1.87500735	-0.04702106
H	3.10752430	0.46854795	-1.52698328

$\tau_{0=C-O-X} = 100^\circ$

	X	Y	Z
C	-0.09415902	-0.18857697	0.00360484
O	-1.17250010	2.11782473	-0.00001089
O	2.46214310	0.03904949	0.11353810
O	-1.22821935	-2.15347062	-0.01644063
H	-2.97892867	1.82717792	-0.03216653
H	3.12522600	0.36415811	-1.55159022

$\tau_{0=C-O-X} = 95^\circ$

	X	Y	Z
C	-0.09210732	-0.18832275	-0.00460187
O	-1.20054902	2.10198938	-0.00351300
O	2.46105411	0.07959000	0.11735376
O	-1.20040188	-2.16862924	-0.01097446
H	-3.00316426	1.78685215	-0.01608321
H	3.14598878	0.24994646	-1.56168604

$\tau_{0=C-O-X} = 90^\circ$

	X	Y	Z
C	-0.09025356	-0.18809562	-0.01287923
O	-1.22392253	2.08818243	-0.00701868
O	2.45891381	0.11573767	0.12008854
O	-1.17642827	-2.18139269	-0.00532182
H	-3.02281465	1.75220078	0.00070352
H	3.16801090	0.12989529	-1.55739227

$\tau_{0=C-O-X} = 85^\circ$

	X	Y	Z
C	-0.08845158	-0.18793564	-0.02085701
O	-1.24432582	2.07562292	-0.01039949
O	2.45582467	0.14920212	0.12163959
O	-1.15461519	-2.19278549	0.00028211
H	-3.03941986	1.72105277	0.01758627
H	3.18981263	0.00817372	-1.53918384

$\tau_{0=C-O-X} = 80^\circ$

	X	Y	Z
C	-0.08654952	-0.18787106	-0.02820023
O	-1.26374569	2.06328723	-0.01354042
O	2.45180628	0.18199694	0.12194329
O	-1.13294118	-2.20389063	0.00561577
H	-3.05471682	1.69074617	0.03402715
H	3.21046202	-0.11074333	-1.50781037

$\tau_{0=C-O-X} = 75^\circ$

	<i>X</i>	<i>Y</i>	<i>Z</i>
C	-0.08439537	-0.18791003	-0.03463017
O	-1.28429104	2.04998105	-0.01633842
O	2.44677045	0.21629557	0.12097408
O	-1.10919019	-2.21578165	0.01048663
H	-3.07049428	1.65832932	0.04948980
H	3.22963690	-0.22230862	-1.46422851

 $\tau_{0=C-O-X} = 70^\circ$

	<i>X</i>	<i>Y</i>	<i>Z</i>
C	-0.08183620	-0.18805470	-0.03993843
O	-1.30813283	2.03435103	-0.01870826
O	2.44050697	0.25439226	0.11874342
O	-1.08100243	-2.22948270	0.01473995
H	-3.08852577	1.62061051	0.06349159
H	3.24762902	-0.32198398	-1.40951569

 $\tau_{0=C-O-X} = 65^\circ$

	<i>X</i>	<i>Y</i>	<i>Z</i>
C	-0.07871712	-0.18830775	-0.04398975
O	-1.33741687	2.01488542	-0.02058450
O	2.43264462	0.29864335	0.11529458
O	-1.04592344	-2.24590413	0.01826261
H	-3.11045721	1.57421523	0.07561624
H	3.26523330	-0.40531915	-1.34479640

 $\tau_{0=C-O-X} = 60^\circ$

	<i>X</i>	<i>Y</i>	<i>Z</i>
C	-0.07488116	-0.18867399	-0.04671564
O	-1.37416547	1.98989736	-0.02192188
O	2.42259431	0.35139844	0.11069545
O	-1.00144223	-2.26575526	0.02098222
H	-3.13766676	1.51563129	0.08551520
H	3.28355232	-0.46800581	-1.27118407

 $\tau_{0=C-O-X} = 55^\circ$

	<i>X</i>	<i>Y</i>	<i>Z</i>
C	-0.07017400	-0.18915474	-0.04810321
O	-1.42011915	1.95752839	-0.02269445
O	2.40948853	0.41485996	0.10503096
O	-0.94508091	-2.28941174	0.02286311
H	-3.17106343	1.44132520	0.09290378
H	3.30372315	-0.50599097	-1.18974130

 $\tau_{0=C-O-X} = 50^\circ$

	<i>X</i>	<i>Y</i>	<i>Z</i>
C	-0.06446282	-0.18973567	-0.04818444
O	-1.47644221	1.91585211	-0.02289382
O	2.39215459	0.49077254	0.09839659

O	-0.87464524	-2.31671901	0.02390121
H	-3.21078625	1.34808138	0.09756231
H	3.32656864	-0.51579904	-1.10145189

$\tau_{0=C-O-X} = 45^\circ$

	X	Y	Z
C	-0.05767364	-0.19037083	-0.04702665
O	-1.54328403	1.86315948	-0.02252677
O	2.36919090	0.57990265	0.09089309
O	-0.78870893	-2.34677159	0.02411863
H	-3.25585217	1.23367112	0.09933973
H	3.35220406	-0.49515905	-1.00720476

$\tau_{0=C-O-X} = 40^\circ$

	X	Y	Z
C	-0.04984830	-0.19097097	-0.04472383
O	-1.61925398	1.79851661	-0.02161277
O	2.33925376	0.68132586	0.08262228
O	-0.68737894	-2.37777198	0.02355829
H	-3.30389226	1.09792420	0.09815707
H	3.37971094	-0.44399841	-0.90779051

$\tau_{0=C-O-X} = 35^\circ$

	X	Y	Z
C	-0.04120729	-0.19141039	-0.04138868
O	-1.70104320	1.72257445	-0.02018188
O	2.30163378	0.79174614	0.07368418
O	-0.57319429	-2.40716177	0.02227905
H	-3.35125381	0.94401072	0.09401227
H	3.40710280	-0.36560822	-0.80390930

$\tau_{0=C-O-X} = 30^\circ$

	X	Y	Z
C	-0.03218124	-0.19156417	-0.03714581
O	-1.78358779	1.63832927	-0.01827342
O	2.25701390	0.90533304	0.06417522
O	-0.45168083	-2.43219973	0.02035164
H	-3.39374807	0.77927712	0.08698579
H	3.43181130	-0.26734739	-0.69618703

$\tau_{0=C-O-X} = 25^\circ$

	X	Y	Z
C	-0.02336630	-0.19136714	-0.03212615
O	-1.86103250	1.55125529	-0.01593510
O	2.20799031	1.01455100	0.05418736
O	-0.33091933	-2.45088498	0.01785551
H	-3.42795423	0.61472850	0.07724571
H	3.45163052	-0.16003738	-0.58519621

$\tau_{0=C-O-X} = 20^\circ$

	<i>X</i>	<i>Y</i>	<i>Z</i>
C	-0.01539828	-0.19085863	-0.02646297
O	-1.92818024	1.46840134	-0.01322266
O	2.15885352	1.11185657	0.04380810
O	-0.21995239	-2.46271644	0.01487660
H	-3.45239359	0.46287153	0.06505200
H	3.46558996	-0.05581888	-0.47147769

 $\tau_{0=C-O-X} = 15^\circ$

	<i>X</i>	<i>Y</i>	<i>Z</i>
C	-0.00880871	-0.19017762	-0.02028936
O	-1.98159546	1.39679339	-0.01019954
O	2.11459381	1.19135572	0.03312094
O	-0.12679146	-2.46874978	0.01150575
H	-3.46777541	0.33493654	0.05075816
H	3.47415131	0.03452168	-0.35556007

 $\tau_{0=C-O-X} = 10^\circ$

	<i>X</i>	<i>Y</i>	<i>Z</i>
C	-0.00394552	-0.18951175	-0.01373603
O	-2.01977238	1.34205270	-0.00693659
O	2.07971453	1.24950682	0.02220600
O	-0.05713647	-2.47094916	0.00783742
H	-3.47622515	0.23903199	0.03480647
H	3.47867571	0.10327791	-0.23797607

 $\tau_{0=C-O-X} = 5^\circ$

	<i>X</i>	<i>Y</i>	<i>Z</i>
C	-0.00098083	-0.18902999	-0.00692324
O	-2.04248422	1.30790248	-0.00350874
O	2.05751089	1.28469795	0.01113863
O	-0.01432703	-2.47132033	0.00396780
H	-3.48011895	0.17998468	0.01765569
H	3.48069362	0.14595992	-0.11928543

 $\tau_{0=C-O-X} = 0^\circ \text{ (1cc)}$

	<i>X</i>	<i>Y</i>	<i>Z</i>
C	0.00000371	0.18885838	0.00000000
O	-2.04998124	-1.29636543	0.00000000
O	2.04995087	-1.29641030	0.00000000
O	0.00002802	2.47127552	0.00000000
H	-3.48121427	-0.16016470	0.00000000
H	3.48120744	-0.16024325	0.00000000

6. Electronic Energies

Table S8. Total energies (in E_h) at FC-CCSD(T)/cc-pVQZ structures

TS1

	RHF	MP2	CCSD	CCSD(T)
cc-pVDZ	-263.5760039	-264.2859961	-264.2879525	-264.3124527
cc-pVTZ	-263.6598483	-264.5519891	-264.5428723	-264.5836235
cc-pVQZ	-263.6801971	-264.6389976	-264.6219528	-264.6670775
cc-pV5Z	-263.6851338	-264.6711473	-264.6475749	

TS2

	RHF	MP2	CCSD	CCSD(T)
cc-pVDZ	-263.5964914	-264.2951575	-264.3009795	-264.3233334
cc-pVTZ	-263.6796110	-264.5611644	-264.5562249	-264.5946505
cc-pVQZ	-263.6997919	-264.6482717	-264.6355181	-264.6782610
cc-pV5Z	-263.7047615	-264.6806100	-264.6613741	-264.7057146

H₂O

	RHF	MP2	CCSD	CCSD(T)
cc-pVDZ	-76.0267685	-76.2284793	-76.2380419	-76.2410826
cc-pVTZ	-76.0570987	-76.3186477	-76.3245538	-76.3322066
cc-pVQZ	-76.0647588	-76.3476392	-76.3507984	-76.3597977
cc-pV5Z	-76.0670121	-76.3585993	-76.3595122	-76.3690401

CO₂

	RHF	MP2	CCSD	CCSD(T)
cc-pVDZ	-187.6506056	-188.1327283	-188.1296276	-188.1476947
cc-pVTZ	-187.7066585	-188.3081868	-188.2986234	-188.3271648
cc-pVQZ	-187.7210597	-188.3679776	-188.3531877	-188.3845642
cc-pV5Z	-187.7243056	-188.3898853	-188.3706493	-188.4030906

Table S9. Total energies (in E_h) for the focal point analyses along the MP2/aug-cc-pVTZ distinguished reaction path (DRP)

$\tau_{0=C-O-X} = 180^\circ$ (1ct)				
	RHF	MP2	CCSD	CCSD(T)
cc-pVDZ	-263.6728824	-264.3511718	-264.3625090	-264.3818713
cc-pVTZ	-263.7560031	-264.6170418	-264.6182584	-264.6532735
cc-pVQZ	-263.7766763	-264.7046617	-264.6982767	-264.7375560
cc-pV5Z	-263.7817499	-264.7370967		
$\tau_{0=C-O-X} = 170^\circ$				
	RHF	MP2	CCSD	CCSD(T)
cc-pVDZ	-263.6724788	-264.3507643	-264.3621180	-264.3814809
cc-pVTZ	-263.7556039	-264.6166380	-264.6178690	-264.6528860
cc-pVQZ	-263.7762754	-264.7042529	-264.6978816	-264.7371624
cc-pV5Z	-263.7813489	-264.7366863		
$\tau_{0=C-O-X} = 160^\circ$				
	RHF	MP2	CCSD	CCSD(T)
cc-pVDZ	-263.6713094	-264.3495742	-264.3609771	-264.3803406
cc-pVTZ	-263.7544487	-264.6154607	-264.6167350	-264.6517561
cc-pVQZ	-263.7751157	-264.7030624	-264.6967324	-264.7360163
cc-pV5Z	-263.7801889	-264.7354913		
$\tau_{0=C-O-X} = 150^\circ$				
	RHF	MP2	CCSD	CCSD(T)
cc-pVDZ	-263.6694934	-264.3477040	-264.3591860	-264.3785476
cc-pVTZ	-263.7526573	-264.6136155	-264.6149604	-264.6499841
cc-pVQZ	-263.7733178	-264.7012010	-264.6949380	-264.7342236
cc-pV5Z	-263.7783905	-264.7336233		
$\tau_{0=C-O-X} = 140^\circ$				
	RHF	MP2	CCSD	CCSD(T)
cc-pVDZ	-263.6672259	-264.3453333	-264.3569179	-264.3762733
cc-pVTZ	-263.7504263	-264.6112863	-264.6127235	-264.6477447
cc-pVQZ	-263.7710798	-264.6988583	-264.6926828	-264.7319659
cc-pV5Z	-263.7761520	-264.7312736		
$\tau_{0=C-O-X} = 130^\circ$				
	RHF	MP2	CCSD	CCSD(T)
cc-pVDZ	-263.6647639	-264.3427220	-264.3544197	-264.3737646
cc-pVTZ	-263.7480139	-264.6087336	-264.6102738	-264.6452860

cc-pVQZ	-263.7686611	-264.6962995	-264.6902212	-264.7294965
cc-pV5Z	-263.7737334	-264.7287101		

$\tau_{0=C-O-X} = 120^\circ$				
	RHF	MP2	CCSD	CCSD(T)
cc-pVDZ	-263.6624081	-264.3401982	-264.3520001	-264.3713341
cc-pVTZ	-263.7457193	-264.6062802	-264.6079168	-264.6429153
cc-pVQZ	-263.7663617	-264.6938483	-264.6878599	-264.7271243
cc-pV5Z	-263.7714349	-264.7262593		

$\tau_{0=C-O-X} = 110^\circ$				
	RHF	MP2	CCSD	CCSD(T)
cc-pVDZ	-263.6604732	-264.3381265	-264.3500017	-264.3693299
cc-pVTZ	-263.7438494	-264.6042767	-264.6059825	-264.6409686
cc-pVQZ	-263.7644887	-264.6918518	-264.6859264	-264.7251816
cc-pV5Z	-263.7695632	-264.7242685		

$\tau_{0=C-O-X} = 100^\circ$				
	RHF	MP2	CCSD	CCSD(T)
cc-pVDZ	-263.6592473	-264.3368504	-264.3487494	-264.3680824
cc-pVTZ	-263.7426755	-264.6030457	-264.6047756	-264.6397586
cc-pVQZ	-263.7633126	-264.6906270	-264.6847205	-264.7239750
cc-pV5Z	-263.7683884	-264.7230508		

$\tau_{0=C-O-X} = 90^\circ$				
	RHF	MP2	CCSD	CCSD(T)
cc-pVDZ	-263.6589434	-264.3366123	-264.3484786	-264.3678288
cc-pVTZ	-263.7423911	-264.6028092	-264.6045100	-264.6395039
cc-pVQZ	-263.7630255	-264.6903920	-264.6844537	-264.7237199
cc-pV5Z	-263.7681024	-264.7228199		

$\tau_{0=C-O-X} = 80^\circ$				
	RHF	MP2	CCSD	CCSD(T)
cc-pVDZ	-263.6596544	-264.3374855	-264.3492704	-264.3686455
cc-pVTZ	-263.7430758	-264.6036279	-264.6052540	-264.6402688
cc-pVQZ	-263.7637058	-264.6912064	-264.6851939	-264.7244807
cc-pV5Z	-263.7687837	-264.7236360		

$\tau_{0=C-O-X} = 70^\circ$

	RHF	MP2	CCSD	CCSD(T)
cc-pVDZ	-263.6613254	-264.3393549	-264.3510289	-264.3704276
cc-pVTZ	-263.7446750	-264.6053887	-264.6069138	-264.6419493
cc-pVQZ	-263.7652978	-264.6929578	-264.6868479	-264.7261539
cc-pV5Z	-263.7703753	-264.7253883		

 $\tau_{0=C-O-X} = 60^\circ$

	RHF	MP2	CCSD	CCSD(T)
cc-pVDZ	-263.6637624	-264.3419569	-264.3535129	-264.3729251
cc-pVTZ	-263.7470056	-264.6078439	-264.6092643	-264.6443094
cc-pVQZ	-263.7676177	-264.6954009	-264.6891925	-264.7285061
cc-pV5Z	-263.7726923	-264.7278319		

 $\tau_{0=C-O-X} = 50^\circ$

	RHF	MP2	CCSD	CCSD(T)
cc-pVDZ	-263.6666684	-264.3449506	-264.3563993	-264.3758108
cc-pVTZ	-263.7497866	-264.6106741	-264.6120038	-264.6470423
cc-pVQZ	-263.7703849	-264.6982195	-264.6919281	-264.7312333
cc-pV5Z	-263.7754538	-264.7306512		

 $\tau_{0=C-O-X} = 40^\circ$

	RHF	MP2	CCSD	CCSD(T)
cc-pVDZ	-263.6696959	-264.3479816	-264.3593441	-264.3787422
cc-pVTZ	-263.7526868	-264.6135460	-264.6148076	-264.6498251
cc-pVQZ	-263.7732689	-264.7010824	-264.6947309	-264.7340140
cc-pV5Z	-263.7783301	-264.7335144		

 $\tau_{0=C-O-X} = 30^\circ$

	RHF	MP2	CCSD	CCSD(T)
cc-pVDZ	-263.6724953	-264.3507242	-264.3620240	-264.3814014
cc-pVTZ	-263.7553703	-264.6161504	-264.6173669	-264.6523559
cc-pVQZ	-263.7759360	-264.7036804	-264.6972912	-264.7365454
cc-pV5Z	-263.7809884	-264.7361124		

 $\tau_{0=C-O-X} = 20^\circ$

	RHF	MP2	CCSD	CCSD(T)
cc-pVDZ	-263.6747516	-264.3529021	-264.3641609	-264.3835174
cc-pVTZ	-263.7575341	-264.6182228	-264.6194128	-264.6543739
cc-pVQZ	-263.7780854	-264.7057484	-264.6993384	-264.7385648
cc-pV5Z	-263.7831296	-264.7381794		

$\tau_{0=C-O-X} = 10^\circ$

	RHF	MP2	CCSD	CCSD(T)
cc-pVDZ	-263.6762144	-264.3543015	-264.3655373	-264.3848789
cc-pVTZ	-263.7589370	-264.6195564	-264.6207330	-264.6556744
cc-pVQZ	-263.7794783	-264.7070789	-264.7006592	-264.7398661
cc-pV5Z	-263.7845165	-264.7395087		

 $\tau_{0=C-O-X} = 0^\circ \text{ (1cc)}$

	RHF	MP2	CCSD	CCSD(T)
cc-pVDZ	-263.6767209	-264.3547840	-264.3660126	-264.3853487
cc-pVTZ	-263.7594228	-264.6200166	-264.6211892	-264.6561235
cc-pVQZ	-263.7799605	-264.7075380	-264.7011156	-264.7403155
cc-pV5Z	-263.7849965	-264.7399673		

7. Focal Point Analyses

Notation: The symbol δ denotes the increment in the energy difference (ΔE_e) with respect to the previous level of theory in the hierarchy RHF → MP2 → CCSD → CCSD(T). Bracketed numbers result from basis set extrapolations (using the specified functions and fit points) or additivity approximations, while unbracketed numbers were explicitly computed. Most of the focal-point tables target $\Delta E_e[\text{CCSD(T)}]$ in the complete basis set limit (NET/CBS LIMIT). The main table involves correlation of valence electrons only. In all cases auxiliary energy terms are appended for zero-point vibrational energy [$\Delta(\text{ZPVE})$] and core electron correlation [$\Delta(\text{core})$]. In some cases small shifts due to the diagonal Born-Oppenheimer correction [$\Delta(\text{DBOC})$] and the mass-velocity and Darwin terms of special relativity [$\Delta(\text{rel})$] are also included. Final energy differences are boldfaced.

Table S10. Focal point analysis of relative energies (in kcal mol⁻¹)

(A) Relative energy of **TS1** with respect to **1cc** conformer

	$\Delta E_e(\text{RHF})$	$+\delta$ [MP2]	$+\delta$ [CCSD]	$+\delta$ [CCSD(T)]	NET
cc-pVDZ	+63.89	-20.93	+5.94	-3.36	[45.54]
cc-pVTZ	+63.28	-20.62	+6.63	-3.80	[45.49]
cc-pVQZ	+63.44	-20.39	+6.86	-3.88	[46.03]
cc-pV5Z	+63.50	-20.28	+6.94	[-3.88]	[46.29]
CBS LIMIT	[+63.53]	[-20.16]	[+7.02]	[-3.88]	[46.52]
FUNCTION	$a+be^{-cx}$	$a+bX^{-3}$	$a+bX^{-3}$	<i>additivity</i>	
X (Fit points) =	(3,4,5)	(4,5)	(4,5)	(4,5)	

FC-CCSD(T)/cc-pVQZ reference geometries

$$\Delta\text{ZPVE} \text{ (harmonic)} = -4.11 \quad \Delta(\text{DBOC}) = +0.01$$

$$\Delta(\text{relativity}) = -0.12 \quad \Delta(\text{core correlation}) = +0.16$$

$$\Delta E_0 = 46.52 - 4.11 + 0.01 - 0.12 + 0.16 = \mathbf{+42.46 \text{ kcal mol}^{-1}}$$

(B) Relative energy of H₂O and CO₂ (isolated) with respect to **1cc** conformer

	$\Delta E_e(\text{RHF})$	$+\delta$ [MP2]	$+\delta$ [CCSD]	$+\delta$ [CCSD(T)]	NET
cc-pVDZ	+0.28	-4.51	+3.11	-1.23	[-2.35]
cc-pVTZ	-1.92	-2.38	+3.20	-0.94	[-2.04]
cc-pVQZ	-2.84	-2.19	+3.46	-0.90	[-2.47]
cc-pV5Z	-3.13	-2.18	+3.64	-0.90	[-2.56]
CBS LIMIT	[-3.29]	[-2.16]	[+3.84]	[-0.90]	[-2.51]
FUNCTION	$a+be^{-cx}$	$a+bX^{-3}$	$a+bX^{-3}$	$a+bX^{-3}$	
X (Fit points) =	(3,4,5)	(4,5)	(4,5)	(4,5)	

FC-CCSD(T)/cc-pVQZ reference geometries

$$\Delta\text{ZPVE} \text{ (harmonic)} = -4.36 \quad \Delta(\text{DBOC}) = +0.03$$

$$\Delta(\text{relativity}) = -0.21 \quad \Delta(\text{core correlation}) = +0.03$$

$$\Delta E_0 = -2.51 - 4.36 + 0.03 - 0.21 + 0.03 = \mathbf{-7.01 \text{ kcal mol}^{-1}}$$

(C) Relative energy of **TS2** with respect to **1cc** conformer

	$\Delta E_e(\text{RHF})$	$+\delta$ [MP2]	$+\delta$ [CCSD]	$+\delta$ [CCSD(T)]	NET
cc-pVDZ	+51.03	-13.82	+3.52	-2.01	[38.71]
cc-pVTZ	+50.88	-13.98	+4.01	-2.34	[38.57]
cc-pVQZ	+51.14	-13.92	+4.16	-2.38	[39.01]
cc-pV5Z	+51.18	-13.90	+4.22	-2.39	[39.12]
CBS LIMIT	[+51.19]	[-13.88]	[+4.27]	[-2.39]	[39.19]
FUNCTION	$a+be^{-cX}$	$a+bX^{-3}$	$a+bX^{-3}$	$a+bX^{-3}$	
X (Fit points) =	(3,4,5)	(4,5)	(4,5)	(4,5)	

FC-CCSD(T)/cc-pVQZ reference geometries

$$\Delta ZPVE \text{ (harmonic)} = -3.00 \quad \Delta(\text{DBOC}) = -0.01$$

$$\Delta(\text{relativity}) = -0.04 \quad \Delta(\text{core correlation}) = +0.05$$

$$\Delta E_0 = 39.19 - 3.00 - 0.01 - 0.04 + 0.05 = \mathbf{+36.19 \text{ kcal mol}^{-1}}$$

Table S11. FPA tables for the energy profile of the **1ct**→**1cc** distinguished reaction path

All energies (in kcal mol⁻¹) are relative to **1ct** ($\tau_{O=C-O-X} = 180^\circ$).

$\tau_{O=C-O-X} = 170^\circ$

	$\Delta E_e(\text{RHF})$	$+\delta \text{ [MP2]}$	$+\delta \text{ [CCSD]}$	$+\delta \text{ [CCSD(T)]}$	NET
cc-pVDZ	+0.25	+0.00	-0.01	+0.00	[+0.24]
cc-pVTZ	+0.25	+0.00	-0.01	+0.00	[+0.24]
cc-pVQZ	+0.25	+0.00	-0.01	+0.00	[+0.25]
cc-pV5Z	+0.25	+0.01	[-0.01]	[-0.00]	[+0.25]
CBS LIMIT	[+0.25]	[+0.01]	[-0.01]	[-0.00]	[+0.25]
FUNCTION	$a+be^{-cX}$	$a+bX^3$	$a+bX^{-3}$	$a+bX^{-3}$	
X (Fit points) =	(3,4,5)	(4,5)	(4,5)	(4,5)	

$$\text{H}_2\text{CO}_3 \quad E_{\text{rel}} = \Delta E_e + \Delta(\text{ZPVE}) + \Delta(\text{core}) = +0.25 + 0.00 + 0.00 = \mathbf{+0.25 \text{ kcal mol}^{-1}}$$

$$\text{HDCO}_3 \quad E_{\text{rel}} = \Delta E_e + \Delta(\text{ZPVE}) + \Delta(\text{core}) = +0.25 + 0.00 + 0.00 = \mathbf{+0.25 \text{ kcal mol}^{-1}}$$

$\tau_{O=C-O-X} = 160^\circ$

	$\Delta E_e(\text{RHF})$	$+\delta \text{ [MP2]}$	$+\delta \text{ [CCSD]}$	$+\delta \text{ [CCSD(T)]}$	NET
cc-pVDZ	+0.99	+0.02	-0.04	+0.00	[+0.96]
cc-pVTZ	+0.98	+0.02	-0.04	+0.00	[+0.95]
cc-pVQZ	+0.98	+0.02	-0.03	+0.00	[+0.97]
cc-pV5Z	+0.98	+0.03	[-0.03]	[-0.00]	[+0.97]
CBS LIMIT	[+0.98]	[+0.03]	[-0.03]	[-0.00]	[+0.97]
FUNCTION	$a+be^{-cX}$	$a+bX^3$	$a+bX^{-3}$	$a+bX^{-3}$	
X (Fit points) =	(3,4,5)	(4,5)	(4,5)	(4,5)	

$$\text{H}_2\text{CO}_3 \quad E_{\text{rel}} = \Delta E_e + \Delta(\text{ZPVE}) + \Delta(\text{core}) = +0.97 - 0.01 + 0.00 = \mathbf{+0.96 \text{ kcal mol}^{-1}}$$

$$\text{HDCO}_3 \quad E_{\text{rel}} = \Delta E_e + \Delta(\text{ZPVE}) + \Delta(\text{core}) = +0.97 - 0.01 + 0.00 = \mathbf{+0.97 \text{ kcal mol}^{-1}}$$

$\tau_{O=C-O-X} = 150^\circ$

	$\Delta E_e(\text{RHF})$	$+\delta \text{ [MP2]}$	$+\delta \text{ [CCSD]}$	$+\delta \text{ [CCSD(T)]}$	NET
cc-pVDZ	+2.13	+0.05	-0.09	+0.00	[+2.09]
cc-pVTZ	+2.10	+0.05	-0.08	-0.01	[+2.06]
cc-pVQZ	+2.11	+0.06	-0.08	+0.00	[+2.09]
cc-pV5Z	+2.11	+0.07	[-0.08]	[-0.00]	[+2.10]
CBS LIMIT	[+2.11]	[+0.08]	[-0.08]	[-0.00]	[+2.11]
FUNCTION	$a+be^{-cX}$	$a+bX^3$	$a+bX^{-3}$	$a+bX^{-3}$	
X (Fit points) =	(3,4,5)	(4,5)	(4,5)	(4,5)	

$$\text{H}_2\text{CO}_3 \quad E_{\text{rel}} = \Delta E_e + \Delta(\text{ZPVE}) + \Delta(\text{core}) = +2.11 - 0.03 + 0.00 = \mathbf{+2.09 \text{ kcal mol}^{-1}}$$

$$\text{HDCO}_3 \quad E_{\text{rel}} = \Delta E_e + \Delta(\text{ZPVE}) + \Delta(\text{core}) = +2.11 - 0.01 + 0.00 = \mathbf{+2.10 \text{ kcal mol}^{-1}}$$

$\tau_{O=C-O-X} = 140^\circ$

	$\Delta E_e(\text{RHF})$	$+\delta \text{ [MP2]}$	$+\delta \text{ [CCSD]}$	$+\delta \text{ [CCSD(T)]}$	NET
cc-pVDZ	+3.55	+0.11	-0.16	+0.00	[+3.51]
cc-pVTZ	+3.50	+0.11	-0.14	+0.00	[+3.47]
cc-pVQZ	+3.51	+0.13	-0.13	+0.00	[+3.51]
cc-pV5Z	+3.51	+0.14	[-0.13]	[-0.00]	[+3.52]
CBS LIMIT	[+3.51]	[+0.15]	[-0.13]	[-0.00]	[+3.53]
FUNCTION	$a+be^{-cX}$	$a+bX^{-3}$	$a+bX^{-3}$	$a+bX^{-3}$	
X (Fit points) =	(3,4,5)	(4,5)	(4,5)	(4,5)	
H₂CO₃	$E_{\text{rel}} = \Delta E_e + \Delta(\text{ZPVE}) + \Delta(\text{core}) = +3.53 - 0.04 + 0.01 = +3.50 \text{ kcal mol}^{-1}$				
HDCO₃	$E_{\text{rel}} = \Delta E_e + \Delta(\text{ZPVE}) + \Delta(\text{core}) = +3.53 - 0.02 + 0.01 = +3.52 \text{ kcal mol}^{-1}$				

$\tau_{O=C-O-X} = 130^\circ$

	$\Delta E_e(\text{RHF})$	$+\delta \text{ [MP2]}$	$+\delta \text{ [CCSD]}$	$+\delta \text{ [CCSD(T)]}$	NET
cc-pVDZ	+5.09	+0.21	-0.23	+0.01	[+5.09]
cc-pVTZ	+5.01	+0.20	-0.20	+0.00	[+5.01]
cc-pVQZ	+5.03	+0.22	-0.19	+0.00	[+5.06]
cc-pV5Z	+5.03	+0.23	[-0.19]	[+0.00]	[+5.07]
CBS LIMIT	[+5.03]	[+0.25]	[-0.19]	[+0.00]	[+5.09]
FUNCTION	$a+be^{-cX}$	$a+bX^{-3}$	$a+bX^{-3}$	$a+bX^{-3}$	
X (Fit points) =	(3,4,5)	(4,5)	(4,5)	(4,5)	
H₂CO₃	$E_{\text{rel}} = \Delta E_e + \Delta(\text{ZPVE}) + \Delta(\text{core}) = +5.09 - 0.04 + 0.01 = +5.05 \text{ kcal mol}^{-1}$				
HDCO₃	$E_{\text{rel}} = \Delta E_e + \Delta(\text{ZPVE}) + \Delta(\text{core}) = +5.09 - 0.02 + 0.01 = +5.08 \text{ kcal mol}^{-1}$				

$\tau_{O=C-O-X} = 120^\circ$

	$\Delta E_e(\text{RHF})$	$+\delta \text{ [MP2]}$	$+\delta \text{ [CCSD]}$	$+\delta \text{ [CCSD(T)]}$	NET
cc-pVDZ	+6.57	+0.31	-0.29	+0.02	[+6.61]
cc-pVTZ	+6.45	+0.30	-0.26	+0.01	[+6.50]
cc-pVQZ	+6.47	+0.31	-0.25	+0.01	[+6.55]
cc-pV5Z	+6.47	+0.33	[-0.25]	[+0.01]	[+6.56]
CBS LIMIT	[+6.47]	[+0.34]	[-0.25]	[+0.01]	[+6.57]
FUNCTION	$a+be^{-cX}$	$a+bX^{-3}$	$a+bX^{-3}$	$a+bX^{-3}$	
X (Fit points) =	(3,4,5)	(4,5)	(4,5)	(4,5)	
H₂CO₃	$E_{\text{rel}} = \Delta E_e + \Delta(\text{ZPVE}) + \Delta(\text{core}) = +6.57 - 0.04 + 0.01 = +6.55 \text{ kcal mol}^{-1}$				
HDCO₃	$E_{\text{rel}} = \Delta E_e + \Delta(\text{ZPVE}) + \Delta(\text{core}) = +6.57 - 0.01 + 0.01 = +6.57 \text{ kcal mol}^{-1}$				

$\tau_{O=C-O-X} = 110^\circ$

	$\Delta E_e(\text{RHF})$	$+\delta \text{ [MP2]}$	$+\delta \text{ [CCSD]}$	$+\delta \text{ [CCSD(T)]}$	NET
cc-pVDZ	+7.79	+0.40	-0.34	+0.02	[+7.87]
cc-pVTZ	+7.63	+0.38	-0.31	+0.02	[+7.72]
cc-pVQZ	+7.65	+0.39	-0.29	+0.02	[+7.77]
cc-pV5Z	+7.65	+0.40	[-0.29]	[+0.02]	[+7.78]
CBS LIMIT	[+7.64]	[+0.42]	[-0.29]	[+0.02]	[+7.79]
FUNCTION	$a+be^{-cX}$	$a+bX^3$	$a+bX^3$	$a+bX^3$	
X (Fit points) =	(3,4,5)	(4,5)	(4,5)	(4,5)	

$$\begin{array}{ll} \text{H}_2\text{CO}_3 & E_{\text{rel}} = \Delta E_e + \Delta(\text{ZPVE}) + \Delta(\text{core}) = +7.79 - 0.03 + 0.01 = \mathbf{+7.77 \text{ kcal mol}^{-1}} \\ \text{HDCO}_3 & E_{\text{rel}} = \Delta E_e + \Delta(\text{ZPVE}) + \Delta(\text{core}) = +7.79 + 0.00 + 0.01 = \mathbf{+7.80 \text{ kcal mol}^{-1}} \end{array}$$

$\tau_{O=C-O-X} = 100^\circ$

	$\Delta E_e(\text{RHF})$	$+\delta \text{ [MP2]}$	$+\delta \text{ [CCSD]}$	$+\delta \text{ [CCSD(T)]}$	NET
cc-pVDZ	+8.56	+0.43	-0.35	+0.02	[+8.65]
cc-pVTZ	+8.36	+0.42	-0.32	+0.02	[+8.48]
cc-pVQZ	+8.39	+0.42	-0.30	+0.02	[+8.52]
cc-pV5Z	+8.38	+0.43	[-0.30]	[+0.02]	[+8.53]
CBS LIMIT	[+8.38]	[+0.44]	[-0.30]	[+0.02]	[+8.53]
FUNCTION	$a+be^{-cX}$	$a+bX^3$	$a+bX^3$	$a+bX^3$	
X (Fit points) =	(3,4,5)	(4,5)	(4,5)	(4,5)	

$$\begin{array}{ll} \text{H}_2\text{CO}_3 & E_{\text{rel}} = \Delta E_e + \Delta(\text{ZPVE}) + \Delta(\text{core}) = +8.53 - 0.01 + 0.01 = \mathbf{+8.54 \text{ kcal mol}^{-1}} \\ \text{HDCO}_3 & E_{\text{rel}} = \Delta E_e + \Delta(\text{ZPVE}) + \Delta(\text{core}) = +8.53 + 0.01 + 0.01 = \mathbf{+8.56 \text{ kcal mol}^{-1}} \end{array}$$

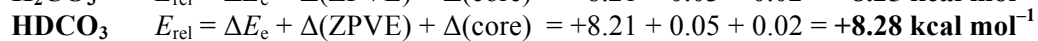
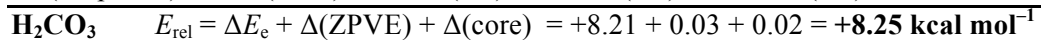
$\tau_{O=C-O-X} = 90^\circ$

	$\Delta E_e(\text{RHF})$	$+\delta \text{ [MP2]}$	$+\delta \text{ [CCSD]}$	$+\delta \text{ [CCSD(T)]}$	NET
cc-pVDZ	+8.75	+0.39	-0.33	+0.01	[+8.81]
cc-pVTZ	+8.54	+0.39	-0.30	+0.01	[+8.64]
cc-pVQZ	+8.57	+0.39	-0.28	+0.01	[+8.68]
cc-pV5Z	+8.56	+0.39	[-0.28]	[+0.01]	[+8.69]
CBS LIMIT	[+8.56]	[+0.40]	[-0.28]	[+0.01]	[+8.69]
FUNCTION	$a+be^{-cX}$	$a+bX^3$	$a+bX^3$	$a+bX^3$	
X (Fit points) =	(3,4,5)	(4,5)	(4,5)	(4,5)	

$$\begin{array}{ll} \text{H}_2\text{CO}_3 & E_{\text{rel}} = \Delta E_e + \Delta(\text{ZPVE}) + \Delta(\text{core}) = +8.69 + 0.01 + 0.02 = \mathbf{+8.71 \text{ kcal mol}^{-1}} \\ \text{HDCO}_3 & E_{\text{rel}} = \Delta E_e + \Delta(\text{ZPVE}) + \Delta(\text{core}) = +8.69 + 0.03 + 0.02 = \mathbf{+8.74 \text{ kcal mol}^{-1}} \end{array}$$

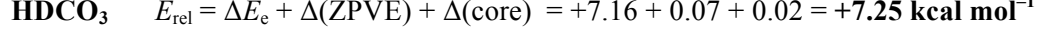
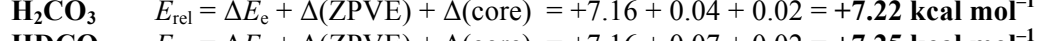
$\tau_{O=C-O-X} = 80^\circ$

	$\Delta E_e(\text{RHF})$	$+\delta \text{ [MP2]}$	$+\delta \text{ [CCSD]}$	$+\delta \text{ [CCSD(T)]}$	NET
cc-pVDZ	+8.30	+0.29	-0.28	-0.01	[+8.30]
cc-pVTZ	+8.11	+0.31	-0.26	+0.00	[+8.16]
cc-pVQZ	+8.14	+0.30	-0.23	+0.00	[+8.20]
cc-pV5Z	+8.14	+0.31	[-0.23]	[-0.00]	[+8.21]
CBS LIMIT	[+8.13]	[+0.32]	[-0.23]	[-0.00]	[+8.21]
FUNCTION	$a+be^{-cX}$	$a+bX^3$	$a+bX^3$	$a+bX^3$	
X (Fit points) =	(3,4,5)	(4,5)	(4,5)	(4,5)	



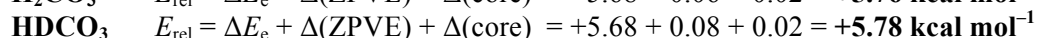
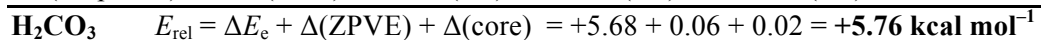
$\tau_{O=C-O-X} = 70^\circ$

	$\Delta E_e(\text{RHF})$	$+\delta \text{ [MP2]}$	$+\delta \text{ [CCSD]}$	$+\delta \text{ [CCSD(T)]}$	NET
cc-pVDZ	+7.25	+0.16	-0.21	-0.02	[+7.18]
cc-pVTZ	+7.11	+0.20	-0.19	-0.01	[+7.11]
cc-pVQZ	+7.14	+0.20	-0.17	-0.02	[+7.15]
cc-pV5Z	+7.14	+0.21	[-0.17]	[-0.02]	[+7.16]
CBS LIMIT	[+7.13]	[+0.22]	[-0.17]	[-0.02]	[+7.16]
FUNCTION	$a+be^{-cX}$	$a+bX^3$	$a+bX^3$	$a+bX^3$	
X (Fit points) =	(3,4,5)	(4,5)	(4,5)	(4,5)	



$\tau_{O=C-O-X} = 60^\circ$

	$\Delta E_e(\text{RHF})$	$+\delta \text{ [MP2]}$	$+\delta \text{ [CCSD]}$	$+\delta \text{ [CCSD(T)]}$	NET
cc-pVDZ	+5.72	+0.06	-0.14	-0.03	[+5.61]
cc-pVTZ	+5.65	+0.13	-0.13	-0.02	[+5.63]
cc-pVQZ	+5.68	+0.13	-0.11	-0.02	[+5.68]
cc-pV5Z	+5.68	+0.13	[-0.11]	[-0.02]	[+5.68]
CBS LIMIT	[+5.68]	[+0.13]	[-0.11]	[-0.02]	[+5.68]
FUNCTION	$a+be^{-cX}$	$a+bX^3$	$a+bX^3$	$a+bX^3$	
X (Fit points) =	(3,4,5)	(4,5)	(4,5)	(4,5)	



$\tau_{O=C-O-X} = 50^\circ$

	$\Delta E_e(\text{RHF})$	$+\delta \text{ [MP2]}$	$+\delta \text{ [CCSD]}$	$+\delta \text{ [CCSD(T)]}$	NET
cc-pVDZ	+3.90	+0.00	-0.07	-0.03	[+3.80]
cc-pVTZ	+3.90	+0.09	-0.07	-0.01	[+3.91]
cc-pVQZ	+3.95	+0.09	-0.06	-0.02	[+3.97]
cc-pV5Z	+3.95	+0.09	[-0.06]	[-0.02]	[+3.97]
CBS LIMIT	[+3.95]	[+0.09]	[-0.06]	[-0.02]	[+3.97]
FUNCTION	$a+be^{-cX}$	$a+bX^3$	$a+bX^3$	$a+bX^3$	
X (Fit points) =	(3,4,5)	(4,5)	(4,5)	(4,5)	

$\text{H}_2\text{CO}_3 \quad E_{\text{rel}} = \Delta E_e + \Delta(\text{ZPVE}) + \Delta(\text{core}) = +3.97 + 0.08 + 0.01 = +4.06 \text{ kcal mol}^{-1}$

$\text{HDCO}_3 \quad E_{\text{rel}} = \Delta E_e + \Delta(\text{ZPVE}) + \Delta(\text{core}) = +3.97 + 0.09 + 0.01 = +4.07 \text{ kcal mol}^{-1}$

$\tau_{O=C-O-X} = 40^\circ$

	$\Delta E_e(\text{RHF})$	$+\delta \text{ [MP2]}$	$+\delta \text{ [CCSD]}$	$+\delta \text{ [CCSD(T)]}$	NET
cc-pVDZ	+2.00	+0.00	-0.02	-0.02	[+1.96]
cc-pVTZ	+2.08	+0.11	-0.03	+0.00	[+2.16]
cc-pVQZ	+2.14	+0.11	-0.02	+0.00	[+2.22]
cc-pV5Z	+2.15	+0.10	[-0.02]	[-0.00]	[+2.22]
CBS LIMIT	[+2.15]	[+0.10]	[-0.02]	[-0.00]	[+2.22]
FUNCTION	$a+be^{-cX}$	$a+bX^3$	$a+bX^3$	$a+bX^3$	
X (Fit points) =	(3,4,5)	(4,5)	(4,5)	(4,5)	

$\text{H}_2\text{CO}_3 \quad E_{\text{rel}} = \Delta E_e + \Delta(\text{ZPVE}) + \Delta(\text{core}) = +2.22 + 0.09 + 0.01 = +2.32 \text{ kcal mol}^{-1}$

$\text{HDCO}_3 \quad E_{\text{rel}} = \Delta E_e + \Delta(\text{ZPVE}) + \Delta(\text{core}) = +2.22 + 0.10 + 0.01 = +2.33 \text{ kcal mol}^{-1}$

$\tau_{O=C-O-X} = 30^\circ$

	$\Delta E_e(\text{RHF})$	$+\delta \text{ [MP2]}$	$+\delta \text{ [CCSD]}$	$+\delta \text{ [CCSD(T)]}$	NET
cc-pVDZ	+0.24	+0.04	+0.02	-0.01	[+0.29]
cc-pVTZ	+0.40	+0.16	+0.00	+0.02	[+0.58]
cc-pVQZ	+0.46	+0.15	+0.00	+0.02	[+0.63]
cc-pV5Z	+0.48	+0.14	[+0.00]	[+0.02]	[+0.64]
CBS LIMIT	[+0.48]	[+0.13]	[+0.00]	[+0.02]	[+0.63]
FUNCTION	$a+be^{-cX}$	$a+bX^3$	$a+bX^3$	$a+bX^3$	
X (Fit points) =	(3,4,5)	(4,5)	(4,5)	(4,5)	

$\text{H}_2\text{CO}_3 \quad E_{\text{rel}} = \Delta E_e + \Delta(\text{ZPVE}) + \Delta(\text{core}) = +0.63 + 0.10 + 0.01 = +0.73 \text{ kcal mol}^{-1}$

$\text{HDCO}_3 \quad E_{\text{rel}} = \Delta E_e + \Delta(\text{ZPVE}) + \Delta(\text{core}) = +0.63 + 0.10 + 0.01 = +0.73 \text{ kcal mol}^{-1}$

$\tau_{O=C-O-X} = 20^\circ$

	$\Delta E_e(\text{RHF})$	$+\delta \text{ [MP2]}$	$+\delta \text{ [CCSD]}$	$+\delta \text{ [CCSD(T)]}$	NET
cc-pVDZ	-1.17	+0.09	+0.05	+0.00	[-1.03]
cc-pVTZ	-0.96	+0.22	+0.02	+0.03	[-0.69]
cc-pVQZ	-0.88	+0.20	+0.02	+0.03	[-0.63]
cc-pV5Z	-0.87	+0.19	[+0.02]	[+0.03]	[-0.63]
CBS LIMIT	[-0.86]	[+0.17]	[+0.02]	[+0.03]	[-0.64]
FUNCTION	$a+be^{-cX}$	$a+bX^3$	$a+bX^3$	$a+bX^3$	
X (Fit points) =	(3,4,5)	(4,5)	(4,5)	(4,5)	
H_2CO_3	$E_{\text{rel}} = \Delta E_e + \Delta(\text{ZPVE}) + \Delta(\text{core}) = -0.64 + 0.10 + 0.01 = \mathbf{-0.54 \text{ kcal mol}^{-1}}$				
HDCO_3	$E_{\text{rel}} = \Delta E_e + \Delta(\text{ZPVE}) + \Delta(\text{core}) = -0.64 + 0.09 + 0.01 = \mathbf{-0.55 \text{ kcal mol}^{-1}}$				

$\tau_{O=C-O-X} = 10^\circ$

	$\Delta E_e(\text{RHF})$	$+\delta \text{ [MP2]}$	$+\delta \text{ [CCSD]}$	$+\delta \text{ [CCSD(T)]}$	NET
cc-pVDZ	-2.09	+0.13	+0.06	+0.01	[-1.89]
cc-pVTZ	-1.84	+0.26	+0.03	+0.05	[-1.51]
cc-pVQZ	-1.76	+0.24	+0.02	+0.05	[-1.45]
cc-pV5Z	-1.74	+0.22	[+0.02]	[+0.05]	[-1.45]
CBS LIMIT	[-1.73]	[+0.20]	[+0.02]	[+0.05]	[-1.46]
FUNCTION	$a+be^{-cX}$	$a+bX^3$	$a+bX^3$	$a+bX^3$	
X (Fit points) =	(3,4,5)	(4,5)	(4,5)	(4,5)	
H_2CO_3	$E_{\text{rel}} = \Delta E_e + \Delta(\text{ZPVE}) + \Delta(\text{core}) = -1.46 + 0.09 + 0.00 = \mathbf{-1.36 \text{ kcal mol}^{-1}}$				
HDCO_3	$E_{\text{rel}} = \Delta E_e + \Delta(\text{ZPVE}) + \Delta(\text{core}) = -1.46 + 0.08 + 0.00 = \mathbf{-1.37 \text{ kcal mol}^{-1}}$				

$\tau_{O=C-O-X} = 0^\circ \text{ (1cc)}$

	$\Delta E_e(\text{RHF})$	$+\delta \text{ [MP2]}$	$+\delta \text{ [CCSD]}$	$+\delta \text{ [CCSD(T)]}$	NET
cc-pVDZ	-2.41	+0.14	+0.07	+0.02	[-2.18]
cc-pVTZ	-2.15	+0.28	+0.03	+0.05	[-1.79]
cc-pVQZ	-2.06	+0.26	+0.02	+0.05	[-1.73]
cc-pV5Z	-2.04	+0.24	[+0.02]	[+0.05]	[-1.73]
CBS LIMIT	[-2.03]	[+0.21]	[+0.02]	[+0.05]	[-1.74]
FUNCTION	$a+be^{-cX}$	$a+bX^3$	$a+bX^3$	$a+bX^3$	
X (Fit points) =	(3,4,5)	(4,5)	(4,5)	(4,5)	
H_2CO_3	$E_{\text{rel}} = \Delta E_e + \Delta(\text{ZPVE}) + \Delta(\text{core}) = -1.74 + 0.09 + 0.00 = \mathbf{-1.64 \text{ kcal mol}^{-1}}$				
HDCO_3	$E_{\text{rel}} = \Delta E_e + \Delta(\text{ZPVE}) + \Delta(\text{core}) = -1.74 + 0.08 + 0.00 = \mathbf{-1.66 \text{ kcal mol}^{-1}}$				

Table S12. Relative energies (E_{rel} , kcal mol $^{-1}$) and projected harmonic vibrational frequencies (cm $^{-1}$) along the **1ct** → **1cc** distinguished reaction path

H₂CO₃

$\tau_{\text{O}=\text{C}-\text{O}-\text{H}}$	arc length	E_{rel}	Projected harmonic frequencies ^a
180°	-2.613	0.00	545, 559, 606, 777, 968, 1159, 1270, 1409, 1881, 3797, 3805
170°	-2.327	0.25	544, 561, 606, 776, 968, 1160, 1269, 1406, 1880, 3797, 3806
160°	-2.041	0.96	543, 567, 606, 773, 967, 1163, 1267, 1399, 1877, 3795, 3809
150°	-1.754	2.09	543, 574, 607, 770, 966, 1168, 1262, 1389, 1872, 3793, 3814
140°	-1.464	3.50	547, 582, 608, 766, 965, 1174, 1253, 1379, 1866, 3789, 3820
130°	-1.168	5.05	551, 591, 611, 764, 963, 1182, 1239, 1372, 1859, 3786, 3826
120°	-0.864	6.55	556, 601, 615, 764, 960, 1191, 1222, 1368, 1853, 3783, 3833
110°	-0.551	7.77	558, 611, 620, 766, 958, 1195, 1211, 1367, 1847, 3781, 3840
100°	-0.229	8.54	559, 620, 623, 769, 957, 1184, 1218, 1370, 1841, 3779, 3846
90°	0.095	8.71	559, 620, 628, 771, 958, 1173, 1230, 1376, 1836, 3779, 3849
80°	0.415	8.25	560, 616, 629, 772, 961, 1166, 1243, 1385, 1832, 3780, 3849
70°	0.726	7.22	559, 611, 627, 773, 966, 1163, 1255, 1396, 1829, 3782, 3845
60°	1.026	5.76	556, 608, 621, 774, 972, 1162, 1265, 1410, 1827, 3785, 3839
50°	1.316	4.06	554, 606, 612, 773, 977, 1163, 1273, 1424, 1827, 3789, 3831
40°	1.598	2.32	552, 600, 608, 772, 980, 1164, 1280, 1438, 1828, 3793, 3823
30°	1.874	0.73	551, 591, 608, 769, 982, 1165, 1284, 1450, 1830, 3796, 3815
20°	2.146	-0.54	550, 584, 606, 768, 983, 1166, 1287, 1459, 1832, 3799, 3808
10°	2.415	-1.36	550, 580, 603, 766, 983, 1166, 1289, 1465, 1834, 3801, 3804
0°	2.683	-1.64	549, 579, 602, 766, 983, 1166, 1289, 1467, 1834, 3801, 3803

HDCO₃

$\tau_{\text{O}=\text{C}-\text{O}-\text{D}}$	arc length	E_{rel}	Projected harmonic frequencies ^a
180°	-3.603	0.00	512, 557, 600, 775, 949, 971, 1202, 1389, 1873, 2769, 3797
170°	-3.208	0.25	512, 559, 600, 773, 951, 971, 1202, 1388, 1872, 2770, 3797
160°	-2.813	0.97	512, 565, 600, 767, 955, 970, 1201, 1384, 1870, 2772, 3795
150°	-2.416	2.10	513, 573, 601, 756, 960, 970, 1199, 1380, 1866, 2776, 3793
140°	-2.015	3.52	518, 582, 603, 742, 963, 974, 1197, 1375, 1861, 2780, 3789
130°	-1.606	5.08	526, 590, 607, 726, 961, 981, 1195, 1370, 1855, 2785, 3786
120°	-1.185	6.57	536, 597, 612, 709, 958, 989, 1194, 1367, 1850, 2790, 3783
110°	-0.754	7.80	547, 603, 617, 693, 955, 996, 1195, 1366, 1845, 2795, 3781
100°	-0.313	8.56	554, 607, 619, 686, 954, 1002, 1198, 1367, 1840, 2800, 3779
90°	0.129	8.74	557, 602, 624, 688, 953, 1105, 1203, 1371, 1836, 2802, 3779
80°	0.567	8.28	555, 593, 627, 700, 954, 1005, 1208, 1377, 1832, 2802, 3780
70°	0.994	7.25	549, 589, 626, 716, 954, 1004, 1213, 1384, 1829, 2799, 3782
60°	1.408	5.78	542, 587, 620, 733, 950, 1005, 1217, 1394, 1826, 2794, 3785
50°	1.809	4.07	537, 587, 611, 746, 942, 1010, 1221, 1404, 1826, 2788, 3789
40°	2.198	2.33	533, 588, 600, 754, 934, 1016, 1224, 1415, 1826, 2782, 3793
30°	2.578	0.73	530, 587, 590, 757, 928, 1023, 1226, 1425, 1826, 2776, 3796
20°	2.949	-0.55	526, 580, 587, 757, 924, 1028, 1227, 1433, 1827, 2771, 3799
10°	3.314	-1.37	523, 575, 585, 756, 921, 1031, 1227, 1438, 1828, 2768, 3801
0°	3.677	-1.66	521, 573, 584, 756, 921, 1032, 1228, 1440, 1828, 2766, 3802

^aMP2/aug-cc-pVTZ level of theory

8. Tunneling Computations

Figure S4. DRP energy curve for the isomerization of **1ct** to **1cc**.

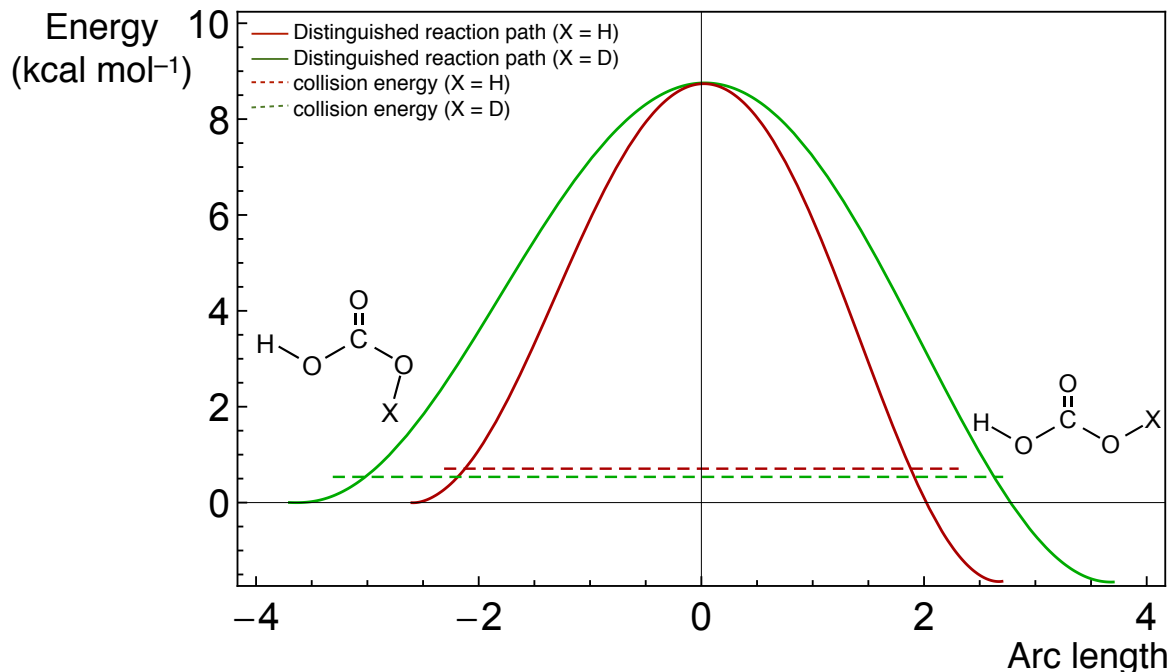


Table S13. Tunneling analysis for **1ct** → **1cc** rotational isomerization of carbonic acid

Tunneling parameters	H ₂ CO ₃	HDCO ₃
Collision energy (ε , kcal mol ⁻¹)	0.71	0.54
Collision frequency (ω_0 , cm ⁻¹)	495	375
Effective barrier (kcal mol ⁻¹)	8.68	8.73
Turning points [(s_1, s_2), a.u.]	(-2.12, 1.88)	(-3.02, 2.63)
Effective barrier frequency (cm ⁻¹)	558 <i>i</i>	411 <i>i</i>
Barrier penetration integral (θ)	19.88	28.18
WKB transmission probability (κ_{WKB})	5.4×10^{-18}	3.3×10^{-25}
WKB half-life (τ_{WKB}^a)	(1.2 h, 72 min)	2900 y
Exact scattering transmission probability (κ)	6.9×10^{-18}	4.1×10^{-25}
Exact scattering half-life (τ) ^a	(0.94, 56 min)	2400 y

^aThe computed half-life was divided by a factor of two due to the degeneracy of the reaction path for internal rotation.

For the estimation of the tunneling rate for the {1,3}H-shift, we mapped out the intrinsic reaction path starting from **TS2** at the MP2/aug-cc-pVTZ level of theory. In order to do so, we employed the Hessian-based predictor-corrector integrator as implemented in the *Gaussian09* electronic structure package. Zero-point vibrational corrections for all modes orthogonal to the reaction path were added to the reaction profile. The latter was refined by computing CCSD(T)/cc-pVQZ energies at all structures along the path. Tunneling probabilities were calculated by numerically integrating the barrier penetration integral and evaluating the WKB equation.

Table S14. Tunneling analysis for **1ct** → **1cc** isomerization via [1,3]H-shift of carbonic acid.

Tunneling parameters	H ₂ CO ₃
Collision energy (ε , kcal mol ⁻¹)	1.82
Collision frequency (ω_0 , cm ⁻¹)	1270
Effective barrier (kcal mol ⁻¹)	36.28
Turning points [(s_1 , s_2), a.u.]	(-2.13, 1.84)
Effective barrier frequency (cm ⁻¹)	1897 <i>i</i>
Barrier penetration integral (θ)	32.10
WKB transmission probability (κ_{WKB})	1.3×10 ⁻²⁸
WKB half-life (τ_{WKB})	(4.4×10 ⁶ y)

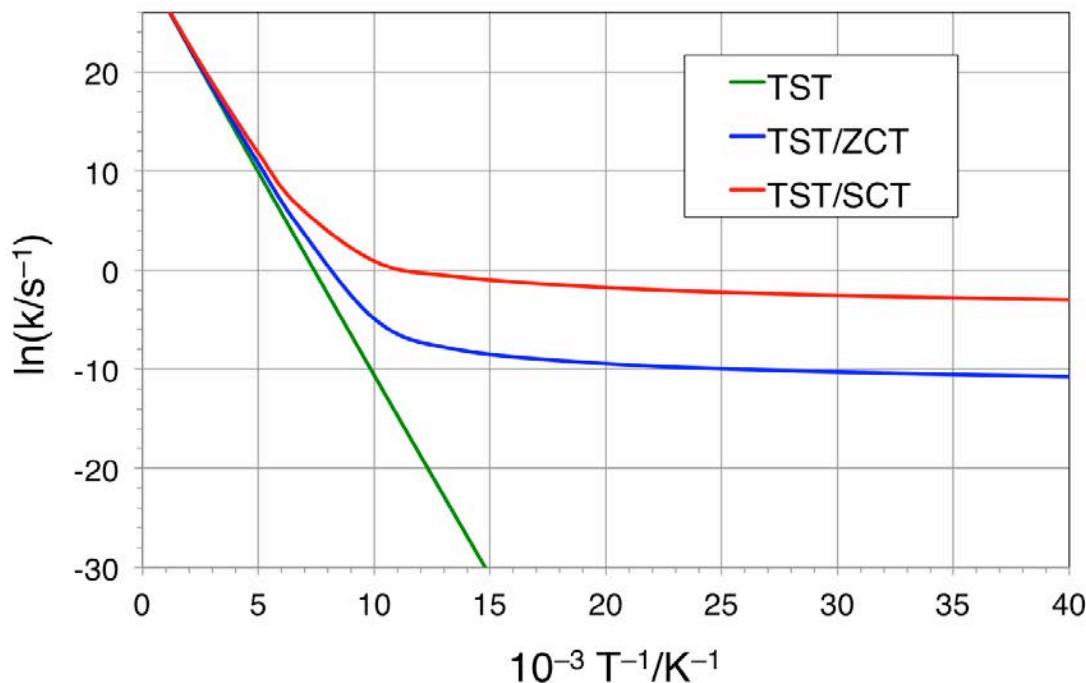
Table S15. Tunneling rates evaluated using different analysis. The FPA/MP2/aug-cc-pVTZ distinguished reaction path is adapted as the one-dimensional potential energy surface.

	ZCT ^a	SCT ^a	WKB ^b	Scattering analysis ^b
Barrier penetration integral (θ)	19.42	15.53		19.88
Transmission probability (k)	1.34×10 ⁻¹⁷	3.22×10 ⁻¹⁴	5.4×10 ⁻¹⁸	6.9×10 ⁻¹⁸
Turning points	(-2.16, 1.86)			(-2.12, 1.88)

^aComputed using the Polyrate 9.3 program.¹⁸

^bThe results reported in the manuscript; computed using our tunneling code in Mathematica.

Figure S5. Arrhenius plot of the rate constants of reaction **1ct** → **1cc**, computed with the Polyrate 9.3 program.¹⁸ The FPA//MP2/aug-cc-pVTZ distinguished reaction path was adapted as the one-dimensional potential energy surface.



9. Vibrational Frequencies

Table S16. IR spectra of *cis,cis*-carbonic acid **1cc** in solid noble gases (band positions in cm^{-1} , intensities^a in parentheses).

Symm.	Approx. Mode	CCSD(T)/cc-pVTZ, unscaled	Ne ^b	Ar ^b	Kr ^b	Xe ^b
a ₁	ν_s (OH)	3846.3 (13.7)	n.o.	n.o.	n.o.	n.o.
b ₂	ν_{as} (OH)	3843.3 (174.4)	3639.7 / 3634.9 (vw) / 3631.5 (w)	3615.3 / 3613.8 / 3609.1 (vw)	3596.2 / 3592.8 (vw)	3575.2 (w)
				1810.6 (vw)	1808.7 (vw)	1804.5 (vw)
a ₁	ν (C=O)	1871.8 (484.2)	1808.1 (s) / 1796.8 (vs)	1791.9 / 1788.0 (vs)	1787.2 (vs)	1780.5 (vs)
b ₂	ν_{as} (OCO) + δ_{as} (HOC)	1501.1 (136.1)	1443.7 (m)	1445.6 / 1437.9 (m)	1443.3 (m)	1439.3 (m)
			1300.4 (w) ^c	1296.5 / 1292.5 (w) ^c	1293.5 / 1288.4 (w) ^c	1290.7 (w) ^c
a ₁	δ_s (HOC) + ν (C=O)	1313.7 (28.1)	1257.8 (w)	1256.0 (w)	1254.3 (w)	1251.7 (w)
b ₂	δ_{as} (HOC) + ν_{as} (OCO)	1183.8 (421.5)	1137.8 (vs)	1136.0 (vs)	1133.8 (vs)	1129.4 (vs)
			1014.0 (vw) ^c	1011.8 / 1005.5 (vw) ^c	1008.9 (vw) ^c	1006.2 (vw) ^c
a ₁	ν_s (OCO)	992.2 (16.2)	959.1 (vw)	966.6 (vw)	n.o.	963.3 (vw)
b ₁	$\delta_{o.o.p.}(CO_3)$	818.2 (52.4)	794.6 (w)	791.6 (m)	790.4 (m)	789.0 (m)
b ₂	δ_{as} (OC=O)	609.3 (51.9)	602.0 (vw)	603.8 / 600.5 (vw).	603.2 (vw)	601.8 (vw)
b ₁	τ (OH)	604.3 (204.8)	570.5 (m)	569.8 / 566.4 / 565.2 (s)	569.0 / 562.1 (s)	568.0 (s)
a ₁	δ (OCO)	550.3 (5.7)	547.5 (vw)	n.o.	n.o.	n.o.
a ₂	τ (OH)	535.4 (0.0)	n.o.	n.o.	n.o.	n.o.

^aComputed intensities in km mol^{-1} , rel. experimental intensities (vw = very weak, w = weak, m = middle, s = strong, vs = very strong);

^bHVFP of di-*tert*.-butyl carbonate; ^cProbably combinational band.

Table S17. IR spectra of *cis,trans*-carbonic acid **1ct** in solid noble gases (band positions in cm^{-1} , intensities^a in parentheses).

Symm.	Approx. Mode	CCSD(T)/cc-pVTZ, unscaled	Ne ^b	Ar ^b	Kr ^b	Xe ^b
a'	ν_s (OH)	3848.1 (87.2)	3634.0 (w)	3610.7 (w)	3591.3 (w)	n.o.
a'	ν_a (OH)	3841.5 (88.3)	3630.4 / 3627.5 (w)	3604.1 (w)	3587.8 / 3584.4 (w)	3561.6
				1843.9 / 1841.5 (m)	1840.8 (w)	1835.6 (w)
a'	ν (C=O)	1922.2 (443.2)	1847.8 / 1835.8 (vs)	1832.2 / 1828.7 (vs)	1827.6 (vs)	1821.0 (vs)
a'	ν (OCO) + δ (HOC)	1443.5 (296.4)	1388.3 (vs)	1391.3 / 1384.5 (vs)	1389.7 / 1388.1 (vs)	1386.3 (vs)
			1333.0 (w) ^c	1332.9 / 1330.1 (w) ^c	1331.7 / 1325.4 (w) ^c	1330.0 (w) ^c
a'	δ (HOC) + ν (C=O)	1293.3 (123.5)	1231.5 (s)	1230.8 / 1228.8 (s)	1226.6 (s) / 1210.8 (vw)	1223.7 (s)
a'	δ (HOC) + ν (OCO)	1182.0 (195.0)	1136.0 (s)	1139.0 (s)	1138.3 (s)	1136.0 (s)
			997.0 (vw) ^c	1000.6 (vw) ^c	999.4 / 986.4 (vw) ^c	997.3 (vw) ^c
a'	ν_s (OCO)	981.1 (39.3)	950.6 / 935.8 (vw)	959.5 / 949.4 (vw)	960.0 / 958.1 (vw)	958.1 (vw)
a''	$\delta_{o.o.p.}$ (CO ₃)	806.5 (30.5)	783.7 (m)	781.6 (m)	780.8 (m)	779.9 (m)
a'	δ (OC=O)	616.8 (9.8)	608.1 (vw)	n.o.	n.o.	609.8 (vw)
a''	τ (O-H)	573.8 (9.6)	n.o.	n.o.	n.o.	n.o.
a'	δ (OCO)	550.7 (28.2)	544.0 (w)	n.o.	n.o.	n.o.
a''	τ (OH)	491.0 (217.3)	474.0 (m)	474.2 / 472.3 / 468.3 (vs)	470.0 / 467.5 (vs)	468.8 (vs)

^aComputed intensities in km mol^{-1} , rel. experimental intensities (vw = very weak, w = weak, m = middle, s = strong, vs = very strong);

^bHVFP of di-*tert*-butyl carbonate; ^cprobably combinational band.

9. Additional References

- (1) Schreiner, P. R.; Wagner, J. P.; Reisenauer, H. P.; Gerbig, D.; Ley, D.; Sarka, J.; Császár, A. G.; Vaughn, A.; Allen, W. D. *J. Am. Chem. Soc.* **2015**, 137, 7828-7834.
- (2) CFOUR, a quantum chemical program package written by J.F. Stanton, J. Gauss, M.E. Harding, P.G. Szalay with contributions from A.A. Auer, R.J. Bartlett, U. Benedikt, C. Berger, D.E. Bernholdt, Y.J. Bomble, L. Cheng, O. Christiansen, M. Heckert, O. Heun, C. Huber, T.-C. Jagau, D. Jonsson, J. Jusélius, K. Klein, W.J. Lauderdale, D.A. Matthews, T. Metzroth, D.P. O'Neill, D.R. Price, E. Prochnow, K. Ruud, F. Schiffmann, W. Schwalbach, S. Stopkowicz, A. Tajti, J. Vázquez, F. Wang, J.D. Watts and the integral packages MOLECULE (J. Almlöf and P.R. Taylor), PROPS (P.R. Taylor), ABACUS (T. Helgaker, H.J. Aa. Jensen, P. Jørgensen, and J. Olsen), and ECP routines by A. V. Mitin and C. van Wüllen. For the current version, see <http://www.cfour.de>.
- (3) Gaussian 09, R. D., Frisch, M. J.; Trucks, G. W.; Schlegel, H. B.; Scuseria, G. E.; Robb, M. A.; Cheeseman, J. R.; Scalmani, G.; Barone, V.; Mennucci, B.; Petersson, G. A.; Nakatsuji, H.; Caricato, M.; Li, X.; Hratchian, H. P.; Izmaylov, A. F.; Bloino, J.; Zheng, G.; Sonnenberg, J. L.; Hada, M.; Ehara, M.; Toyota, K.; Fukuda, R.; Hasegawa, J.; Ishida, M.; Nakajima, T.; Honda, Y.; Kitao, O.; Nakai, H.; Vreven, T.; Montgomery, J. A., Jr.; Peralta, J. E.; Ogliaro, F.; Bearpark, M.; Heyd, J. J.; Brothers, E.; Kudin, K. N.; Staroverov, V. N.; Kobayashi, R.; Normand, J.; Raghavachari, K.; Rendell, A.; Burant, J. C.; Iyengar, S. S.; Tomasi, J.; Cossi, M.; Rega, N.; Millam, N. J.; Klene, M.; Knox, J. E.; Cross, J. B.; Bakken, V.; Adamo, C.; Jaramillo, J.; Gomperts, R.; Stratmann, R. E.; Yazev, O.; Austin, A. J.; Cammi, R.; Pomelli, C.; Ochterski, J. W.; Martin, R. L.; Morokuma, K.; Zakrzewski, V. G.; Voth, G. A.; Salvador, P.; Dannenberg, J. J.; Dapprich, S.; Daniels, A. D.; Farkas, Ö.; Foresman, J. B.; Ortiz, J. V.; Cioslowski, J.; Fox, D. J. Gaussian, Inc., Wallingford CT, 2009.
- (4) Raghavachari, K.; Trucks, G. W.; Pople, J. A.; Head-Gordon, M. *Chem. Phys. Lett.* **1989**, 157, 479-483.
- (5) Bartlett, R. J.; Watts, J. D.; Kucharski, S. A.; Noga, J. *Chem. Phys. Lett.* **1990**, 165, 513-522.
- (6) Erratum to ref (5): R. J. Bartlett, J. D. Watts, S. A. Kucharski, J. Noga *Chem. Phys. Lett.* **1990**, 167, 609.
- (7) Crawford, T. D.; Schaefer, H. F. In *Rev. Comput. Chem.*; John Wiley & Sons, Inc.: 2007, p 33-136.
- (8) Császár, A. G.; Allen, W. D.; Schaefer, H. F. *J. Chem. Phys.* **1998**, 108, 9751-9764.
- (9) Császár, A.; Tarczay, G.; Leininger, M.; Polyansky, O.; Tennyson, J.; Allen, W. In *Spectroscopy from Space*; Demaison, J., Sarka, K., Cohen, E., Eds.; Springer Netherlands: 2001; Vol. 20, p 317-339.
- (10) Dunning, T. H. *J. Chem. Phys.* **1989**, 90, 1007-1023.
- (11) Woon, D. E.; Dunning, T. H. *J. Chem. Phys.* **1995**, 103, 4572-4585.
- (12) Feller, D. *J. Chem. Phys.* **1993**, 98, 7059-7071.
- (13) Halkier, A.; Helgaker, T.; Jørgensen, P.; Klopper, W.; Koch, H.; Olsen, J.; Wilson, A. K. *Chem. Phys. Lett.* **1998**, 286, 243-252.
- (14) Helgaker, T.; Klopper, W.; Koch, H.; Noga, J. *J. Chem. Phys.* **1997**, 106, 9639-9646.
- (15) Klopper, W. *J. Comput. Chem.* **1997**, 18, 20-27.

- (16) Handy, N. C.; Yamaguchi, Y.; Schaefer, H. F. *J. Chem. Phys.* **1986**, *84*, 4481-4484.
- (17) Allen, W. D.; Bodi, A.; Szalay, V.; Császár, A. G. *J. Chem. Phys.* **2006**, *124*, 224310.
- (18) Jingjing Zheng, Shuxia Zhang, Benjamin J. Lynch, José C. Corchado, Yao-Yuan Chuang, Patton L. Fast, Wei-Ping Hu, Yi-Ping Liu, Gillian C. Lynch, Kiet A. Nguyen, Charles F. Jackels, Antonio Fernandez Ramos, Benjamin A. Ellingson, Vasilios S. Melissas, Jordi Villà, Ivan Rossi, Elena. L. Coitiño, Jingzhi Pu, Titus V. Albu, Artur Ratkiewicz, Rozeanne Steckler, Bruce C. Garrett, Alan D. Isaacson, and Donald G. Truhlar *Department of Chemistry and Supercomputing Institute, University of Minnesota, Minneapolis, Minnesota 55455.*